Analysis of Electric Machinery and Drive Systems

SECOND EDITION

Paul C. Krause
Oleg Wasynczuk
Scott D. Sudhoff

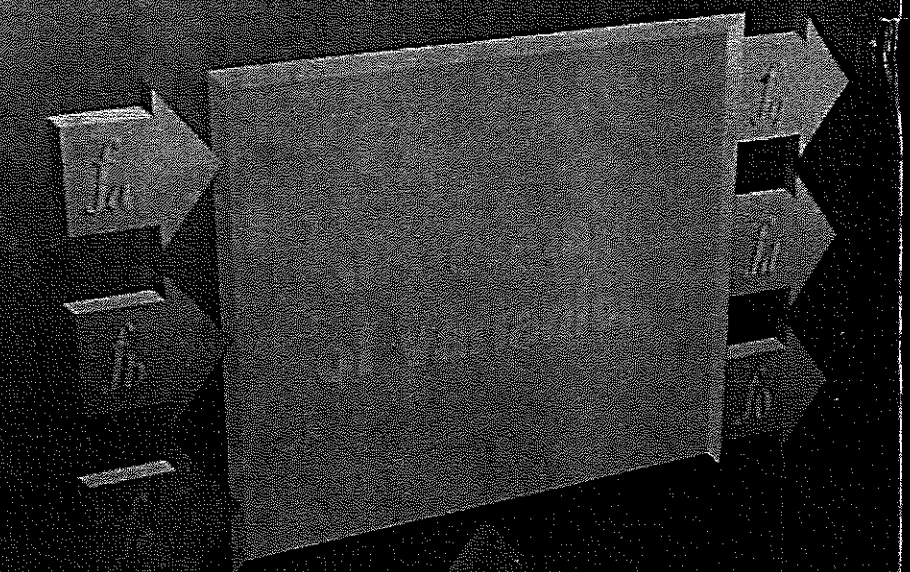

IEEE SERIES ON POWER ENGINEERING

Mohamed E. El-Hawary, *Series Editor*

ANALYSIS OF ELECTRIC MACHINERY AND DRIVE SYSTEMS

Second Edition

PAUL C. KRAUSE
OLEG WASYNCZUK
SCOTT D. SUDHOFF
Purdue University

IEEE Power Engineering Society, *Sponsor*

IEEE Press Power Engineering Series
Mohamed E. El-Hawary, *Series Editor*

IEEE
PRESS

WILEY-
INTERSCIENCE

A JOHN WILEY & SONS, INC. PUBLICATION

This book is printed on acid-free paper. ♾

For ordering and customer service, call 1-800-CALL WILEY.

Library of Congress Cataloging-in-Publication is available.

ISBN 0-471-14326-X

Printed in the United States of America.

13 14 15 16 17 18 19 20

CONTENTS

PREFACE

The first edition of this book was written by Paul C. Krause and published in 1986 by McGraw-Hill. Eight years later the same book was republished by IEEE Press with Oleg Wasynczuk and Scott D. Sudhoff added as co-authors. The focus of the first edition was the analysis of electric machines using reference frame theory, wherein the concept of the arbitrary reference frame was emphasized. Not only has this approach been embraced by the vast majority of electric machine analysts, it has also become the approach used in the analysis of electric drive systems. The use of reference-frame theory to analyze the complete drive system (machine, converter, and control) was not emphasized in the first edition. The goal of this edition is to fill this void and thereby meet the need of engineers whose job it is to analyze and design the complete drive system. For this reason the words "and Drive Systems" have been added to the title.

Although some of the material has been rearranged or revised, and in some cases eliminated, such as 3-phase symmetrical components, most of the material presented in the first ten chapters were taken from the original edition. For the most part, the material in Chapters 11–15 on electric drive systems is new. In particular, the analysis of converters used in electric drive systems is presented in Chapters 11 and 13 while dc, induction, and brushless dc motor drives are analyzed in Chapters 12, 14, and 15, respectively.

Central to the analysis used in this text is the transformation to the arbitrary reference frame. All real and complex transformations used in machine and drive analyses can be shown to be special cases of this general transformation. The modern electric machine and drive analyst must understand reference frame theory. For this reason, the complete performance of all electric machines and drives considered are illustrated by computer traces wherein variables are often portrayed in different

frames of reference so that the student is able to appreciate the advantages and significance of the transformation used.

The material presented in this text can be used most beneficially if the student has had an introductory course in electric machines. However, a senior would be comfortable using this textbook as a first course. For this purpose, considerable time should be devoted to the basic principles discussed in Chapter 1, perhaps some of Chapter 2 covering basic dc machines, most of Chapter 3 covering reference frame theory, and the beginning sections of Chapters 4, 5, and 6 covering induction, synchronous, and brushless dc machines.

Some of the material that would be of interest only to the electric power engineer has been reduced or eliminated from that given in the first edition. However, the material found in the final sections in Chapters 4 and 5 on induction and synchronous machines as well as operational impedances (Chapter 7), and reduced-order modeling (Chapter 9) provide an excellent background for the power utility engineer.

We would like to acknowledge the efforts and assistance of the reviewers, in particular Mohamed E. El-Hawary, and the staff of IEEE Press and John Wiley & Sons.

PAUL C. KRAUSE
OLEG WASYNCZUK
SCOTT D. SUDHOFF

West Lafayette, Indiana
November 2001

Chapter 3

REFERENCE-FRAME THEORY

3.1 INTRODUCTION

The voltage equations that describe the performance of induction and synchronous machines were established in Chapter 1. We found that some of the machine inductances are functions of the rotor speed, whereupon the coefficients of the differential equations (voltage equations) that describe the behavior of these machines are time-varying except when the rotor is stalled. A change of variables is often used to reduce the complexity of these differential equations. There are several changes of variables that are used, and it was originally thought that each change of variables was different and therefore they were treated separately [1–4]. It was later learned that all changes of variables used to transform real variables are contained in one [5,6]. This general transformation refers machine variables to a frame of reference that rotates at an arbitrary angular velocity. All known real transformations are obtained from this transformation by simply assigning the speed of the rotation of the reference frame.

In this chapter this transformation is set forth and, because many of its properties can be studied without the complexities of the machine equations, it is applied to the equations that describe resistive, inductive, and capacitive circuit elements. By this approach, many of the basic concepts and interpretations of this general transformation are readily and concisely established. Extending the material presented in this chapter to the analysis of ac machines is straightforward involving a minimum of trigonometric manipulations.

3.2 BACKGROUND

In the late 1920s, R. H. Park [1] introduced a new approach to electric machine analysis. He formulated a change of variables which, in effect, replaced the variables

(voltages, currents, and flux linkages) associated with the stator windings of a synchronous machine with variables associated with fictitious windings rotating with the rotor. In other words, he transformed, or referred, the stator variables to a frame of reference fixed in the rotor. Park's transformation, which revolutionized electric machine analysis, has the unique property of eliminating all time-varying inductances from the voltage equations of the synchronous machine which occur due to (1) electric circuits in relative motion and (2) electric circuits with varying magnetic reluctance.

In the late 1930s, H. C. Stanley [2] employed a change of variables in the analysis of induction machines. He showed that the time-varying inductances in the voltage equations of an induction machine due to electric circuits in relative motion could be eliminated by transforming the variables associated with the rotor windings (rotor variables) to variables associated with fictitious stationary windings. In this case the rotor variables are transformed to a frame reference fixed in the stator.

G. Kron [3] introduced a change of variables that eliminated the position or time-varying mutual inductances of a symmetrical induction machine by transforming both the stator variables and the rotor variables to a reference frame rotating in synchronism with the rotating magnetic field. This reference frame is commonly referred to as the synchronously rotating reference frame.

D. S. Brereton et al. [4] employed a change of variables that also eliminated the time-varying inductances of a symmetrical induction machine by transforming the stator variables to a reference frame fixed in the rotor. This is essentially Park's transformation applied to induction machines.

Park, Stanley, Kron, and Brereton et al. developed changes of variables, each of which appeared to be uniquely suited for a particular application. Consequently, each transformation was derived and treated separately in literature until it was noted in 1965 [5] that all known real transformations used in induction machine analysis are contained in one general transformation that eliminates all time-varying inductances by referring the stator and the rotor variables to a frame of reference that may rotate at any angular velocity or remain stationary. All known real transformations may then be obtained by simply assigning the appropriate speed of rotation, which may in fact be zero, to this so-called *arbitrary reference frame*. It is interesting to note that this transformation is sometimes referred to as the "generalized rotating real transformation," which may be somewhat misleading because the reference frame need not rotate. In any event, we will refer to it as the arbitrary reference frame as did the originators [5]. Later, it was noted that the stator variables of a synchronous machine could also be referred to the arbitrary reference frame [6]. However, we will find that the time-varying inductances of a synchronous machine are eliminated only if the reference frame is fixed in the rotor (Park's transformation); consequently the arbitrary reference frame does not offer the advantages in the analysis of the synchronous machines that it does in the case of induction machines.

Chapter 6

THEORY OF BRUSHLESS dc MACHINES

6.1 INTRODUCTION

The brushless dc motor is becoming widely used as a small horsepower control motor. This device has the physical appearance of a 3-phase permanent magnet synchronous machine that is supplied from an inverter that converts a dc voltage to 3-phase alternating-current (ac) voltages with frequency corresponding instantaneously to the rotor speed. The inverter–machine combination has the terminal and output (T_e vs. ω_r) characteristics resembling those of a dc shunt machine during motor operation; hence the name *brushless dc motor*. In this brief chapter, equations are derived which describe the operation of a brushless dc machine. The operation of brushless dc motor drives is considered in Chapter 15. In this chapter we look at the performance of the brushless dc motor with balanced 3-phase applied stator voltage with frequency corresponding to the rotor speed. This allows us to become familiar with the salient operating features of the inverter–motor combination without becoming involved with the harmonics of the phase voltages that occur due to the switching of the inverter.

6.2 VOLTAGE AND TORQUE EQUATIONS IN MACHINE VARIABLES

A 2-pole, brushless dc machine is depicted in Fig. 6.2-1. It has 3-phase, wye-connected stator windings and a permanent magnet rotor. It is a synchronous machine. The stator windings are identical windings displaced 120°, each with N_s equivalent turns and resistance r_s. For our analysis we will assume that the stator windings are

sinusoidally distributed. The three sensors shown in Fig. 6.2-1 are Hall effect devices. When the north pole is under a sensor, its output is nonzero; with a south pole under the sensor, its output is zero. In most applications the stator is supplied from an inverter that is switched at a frequency corresponding to the rotor speed. The states of the three sensors are used to determine the switching logic for the inverter.

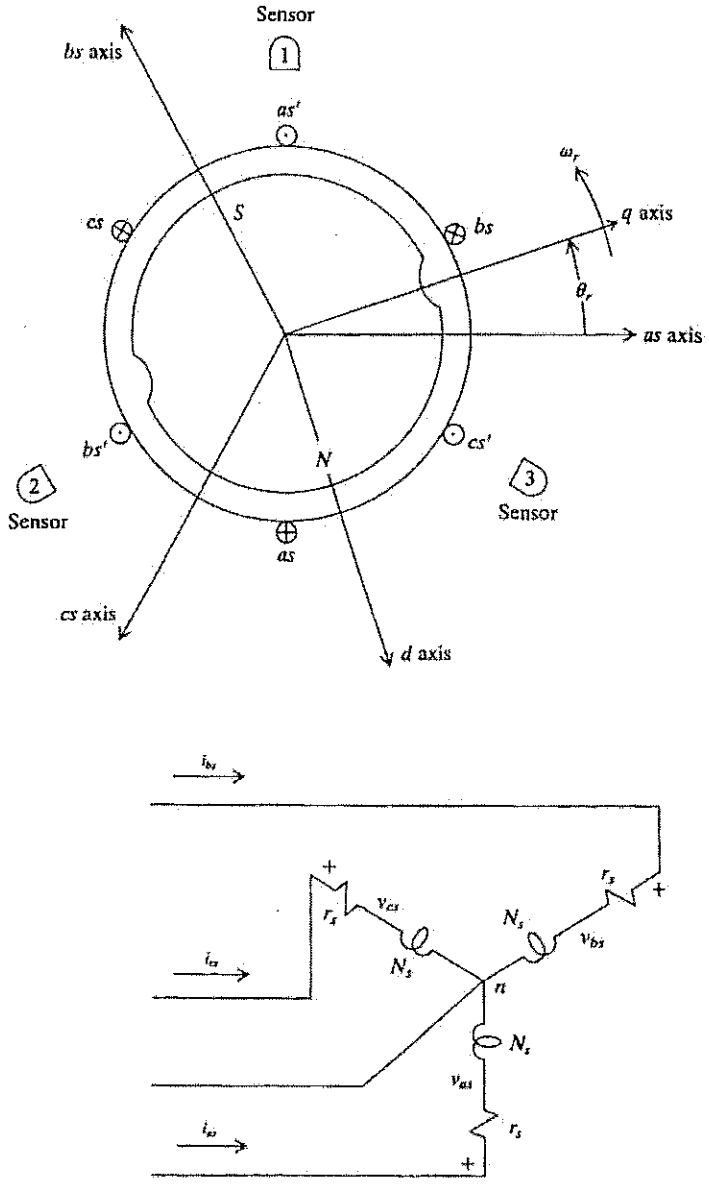

Figure 6.2-1 Two-pole, 3-phase brushless dc machine.

In the actual machine the sensors are not positioned over the rotor as shown in Fig. 6.2-1. Instead they are placed over a ring that is mounted on the shaft external to the stator windings and magnetized as the rotor. We will return to these sensors and the role they play later in this analysis. It is first necessary to establish the voltage and torque equations that can be used to describe the behavior of the permanent magnet synchronous machine.

The voltage equations in machine variables are

$$\mathbf{v}_{abcs} = \mathbf{r}_s \mathbf{i}_{abcs} + p\boldsymbol{\lambda}_{abcs} \tag{6.2-1}$$

where

$$(\mathbf{f}_{abcs})^T = [f_{as} \quad f_{bs} \quad f_{cs}] \tag{6.2-2}$$

$$\mathbf{r}_s = \text{diag}[r_s \quad r_s \quad r_s] \tag{6.2-3}$$

The flux linkages may be written

$$\boldsymbol{\lambda}_{abcs} = \mathbf{L}_s \mathbf{i}_{abcs} + \boldsymbol{\lambda}'_m \tag{6.2-4}$$

where $\mathbf{L}_s$ may be written from (1.5-25)–(1.5-27) and (1.5-29)–(1.5-31) or directly from (5.2-8). Also,

$$\boldsymbol{\lambda}'_m = \lambda'_m \begin{bmatrix} \sin\theta_r \\ \sin\left(\theta_r - \frac{2\pi}{3}\right) \\ \sin\left(\theta_r + \frac{2\pi}{3}\right) \end{bmatrix} \tag{6.2-5}$$

where λ'_m is the amplitude of the flux linkages established by the permanent magnet as viewed from the stator phase windings. In other words the magnitude of $p\boldsymbol{\lambda}'_m$ would be the open-circuit voltage induced in each stator phase winding. Damper windings are neglected because the permanent magnet is a poor electrical conductor and the eddy currents that flow in the nonmagnetic materials securing the magnets are small. Hence, large armature currents can be tolerated without significant demagnetization. We have assumed by (6.2-5) that the voltages induced in the stator windings by the permanent magnet are constant-amplitude sinusoidal voltages. For nonsinusoidal induced voltages see references 1 and 2.

The expression for the electromagnetic torque may be written in machine variables from (5.3-4) by letting $\lambda'_m = L_{md} i'_{fd}$. Thus

$$\begin{aligned} T_e = \left(\frac{P}{2}\right)\Bigg\{ & \frac{(L_{md} - L_{mq})}{3}\Bigg[\left(i_{as}^2 - \frac{1}{2}i_{bs}^2 - \frac{1}{2}i_{cs}^2 - i_{as}i_{bs} - i_{as}i_{cs} + 2i_{bs}i_{cs}\right)\sin 2\theta_r \\ & + \frac{\sqrt{3}}{2}(i_{bs}^2 i_{cs}^2 - 2i_{as}i_{bs} + 2i_{as}i_{cs})\cos 2\theta_r\Bigg] \\ & + \lambda'_m\left[\left(i_{as} - \frac{1}{2}i_{bs} - \frac{1}{2}i_{cs}\right)\cos\theta_r + \frac{\sqrt{3}}{2}(i_{bs} - i_{cs})\sin\theta_r\right]\Bigg\} \end{aligned} \tag{6.2-6}$$

where L_{mq} and L_{md} are defined by (5.2-11) and (5.2-12), respectively. The above expression for torque is positive for motor action. The torque and speed may be related as

$$T_e = J\left(\frac{2}{P}\right)p\omega_r + B_m\left(\frac{2}{P}\right)\omega_r + T_L \tag{6.2-7}$$

where J is kg·m^2 ; it is the inertia of the rotor and the connected load. Because we will be concerned primarily with motor action, the torque T_L is positive for a torque load. The constant B_m is a damping coefficient associated with the rotational system of the machine and the mechanical load. It has the units N·m·s per radian of mechanical rotation, and it is generally small and often neglected.

6.3 VOLTAGE AND TORQUE EQUATIONS IN ROTOR REFERENCE-FRAME VARIABLES

The voltage equations in the rotor reference frame may be written directly from Section 3.4 with $\omega = \omega_r$ or from (5.5-1) with the direction of positive stator currents into the machine.

$$\mathbf{v}^r_{qd0s} = \mathbf{r}_s\mathbf{i}^r_{qd0s} + \omega_r\boldsymbol{\lambda}^r_{dqs} + p\boldsymbol{\lambda}^r_{qd0s} \tag{6.3-1}$$

where

$$\tag{6.3-2}$$

$$\begin{bmatrix} 0 \\ 0 \\ L_{ls} \end{bmatrix}\begin{bmatrix} i^r_{qs} \\ i^r_{ds} \\ i_{0s} \end{bmatrix} + \lambda'^r_m\begin{bmatrix} 0 \\ 1 \\ 0 \end{bmatrix} \tag{6.3-3}$$

To be consistent with our previous notation, we have added the superscript r to λ'_m. In expanded form we have

$$v^r_{qs} = r_s i^r_{qs} + \omega_r\lambda^r_{ds} + p\lambda^r_{qs} \tag{6.3-4}$$

$$v^r_{ds} = r_s i^r_{ds} - \omega_r\lambda^r_{qs} + p\lambda^r_{ds} \tag{6.3-5}$$

$$v_{0s} = r_s i_{0s} + p\lambda_{0s} \tag{6.3-6}$$

where

$$\lambda^r_{qs} = L_q i^r_{qs} \tag{6.3-7}$$

$$\lambda^r_{ds} = L_d i^r_{ds} + \lambda'^r_m \tag{6.3-8}$$

$$\lambda_{0s} = L_{ls} i_{0s} \tag{6.3-9}$$

where $L_q = L_{ls} + L_{mq}$ and $L_d = L_{ls} + L_{md}$.

Substituting (6.3-7)–(6.3-9) into (6.3-4)–(6.3-6) and because $p\lambda'^{r}_{m} = 0$, we can write

$$v^{r}_{qs} = (r_s + pL_q)i^{r}_{qs} + \omega_r L_d i^{r}_{ds} + \omega_r \lambda'^{r}_{m} \tag{6.3-10}$$

$$v^{r}_{ds} = (r_s + pL_d)i^{r}_{ds} - \omega_r L_q i^{r}_{qs} \tag{6.3-11}$$

$$v_{0s} = (r_s + pL_{ls})i_{0s} \tag{6.3-12}$$

The expression for electromagnetic torque may be written from (5.6-9) as

$$T_e = \left(\frac{3}{2}\right)\left(\frac{P}{2}\right)(\lambda^{r}_{ds}i^{r}_{qs} - \lambda^{r}_{qs}i^{r}_{ds}) \tag{6.3-13}$$

Substituting (6.3-7) and (6.3-8) into (6.3-13) yields

$$T_e = \left(\frac{3}{2}\right)\left(\frac{P}{2}\right)[\lambda'^{r}_{m}i^{r}_{qs} + (L_d - L_q)i^{r}_{qs}i^{r}_{ds}] \tag{6.3-14}$$

The electromagnetic torque is positive for motor action.

As pointed out in the previous section, the state of the sensors provides us with information regarding the position of the poles and thus the position of the q and d axes. In other words, when the machine is supplied from an inverter, it is possible, by controlling the firing of the inverter, to change the values of v^{r}_{qs} and v^{r}_{ds}. Recall that θ_r in the transformation equation to the rotor reference frame can be written as

$$\omega_r = \frac{d\theta_r}{dt} \tag{6.3-15}$$

For purposes of discussion, let us assume that the applied stator voltages are sinusoidal so that

$$v_{as} = \sqrt{2}v_s \cos\theta_{ev} \tag{6.3-16}$$

$$v_{bs} = \sqrt{2}v_s \cos\left(\theta_{ev} - \frac{2\pi}{3}\right) \tag{6.3-17}$$

$$v_{cs} = \sqrt{2}v_s \cos\left(\theta_{ev} + \frac{2\pi}{3}\right) \tag{6.3-18}$$

When the machine is supplied from an inverter, the stator voltages will have a stepped waveform. Nevertheless, (6.3-16)–(6.3-18) may be considered as the fundamental components of these stepped phase voltages. Also,

$$\omega_e = \frac{d\theta_{ev}}{dt} \tag{6.3-19}$$

The brushless dc machine is, by definition, a device where the frequency of the fundamental component of the applied stator voltages corresponds to the speed of the rotor, and we understand that this is accomplished by appropriately firing the inverter supplying (driving) the machine. Hence, in a brushless dc machine, ω_e in (6.3-19) is ω_r; and if (6.3-16)–(6.3-18) are substituted into $\mathbf{K}_s^r$, we obtain

$$v_{qs}^r = \sqrt{2}v_s \cos\phi_v \tag{6.3-20}$$

$$v_{ds}^r = -\sqrt{2}v_s \sin\phi_v \tag{6.3-21}$$

where

$$\phi_v = \theta_{ev} - \theta_r \tag{6.3-22}$$

Now, because $\omega_r = \omega_e$ at all times, ϕ_v is a constant during steady-state operation or is changed by advancing or retarding the firing of the inverter relative to the rotor position. In other words, we can, at any time, instantaneously adjust ϕ_v by appropriate firing of the inverter, thereby changing the phase relationship between the fundamental component of the 3-phase stator voltages and the rotor (permanent magnet). In most applications, however, ϕ_v is fixed at zero so that as far as the fundamental component is concerned, v_{ds}^r is always zero and $v_{qs}^r = \sqrt{2}v_s$.

In Section 2.6 the time-domain block diagrams and the state equations were derived for a dc machine. By following the same procedure, the time-domain diagram and state equations can be established for the brushless dc machine directly from the equations given above. Because this essentially is a repeat of the work in Section 2.6, the development is left as an exercise for the readers.

6.4 ANALYSIS OF STEADY-STATE OPERATION

For steady-state operation with balanced, sinusoidal applied stator voltages, (6.3-10) and (6.3-11) may be written as

$$V_{qs}^r = r_s I_{qs}^r + \omega_r L_d I_{ds}^r + \omega_r \lambda_m^{\prime r} \tag{6.4-1}$$

$$V_{ds}^r = r_s I_{ds}^r - \omega_r L_q I_{qs}^r \tag{6.4-2}$$

where uppercase letters denote steady-state (constant) quantities. It is clear that $\lambda_m^{\prime r}$ is always constant. The steady-state torque is expressed from (6.3-14) with uppercase letters as

$$T_e = \left(\frac{3}{2}\right)\left(\frac{P}{2}\right)[\lambda_m^{\prime r} I_{qs}^r + (L_d - L_q) I_{qs}^r I_{ds}^r] \tag{6.4-3}$$

It is possible to establish a phasor voltage equation from (6.4-1) and (6.4-2) similar to that for the synchronous machine. For this purpose let us write (6.3-22) as

$$\theta_{ev} = \theta_r + \phi_v \tag{6.4-4}$$

For steady-state operation ϕ_v is constant and represents the angular displacement between the peak value of the fundamental component of v_{as} and the q axis fixed in the rotor. If we reference the phasors to the q axis and let it be along the positive real axis of the "stationary" phasor diagram, then ϕ_v becomes the phase angle of $\bar{V}_{as}$ and we can write

$$\bar{V}_{as} = V_s e^{j\phi_v} = V_s \cos\phi_v + jV_s \sin\phi_v \tag{6.4-5}$$

Comparing (6.4-5) with (6.3-20) and (6.3-21), we see that

$$\sqrt{2}\bar{V}_{as} = V^r_{qs} - jV^r_{ds} \tag{6.4-6}$$

If we go back and write equations for the 3-phase currents similar to (6.3-16)–(6.3-18) in terms of θ_{ei}, then (6.3-22) would be in terms of θ_{ei} and ϕ_i rather than θ_{ev} and ϕ_v; however, we would arrive at a similar relation for current as (6.4-6). In particular,

$$\sqrt{2}\bar{I}_{as} = I^r_{qs} - jI^r_{ds} \tag{6.4-7}$$

and

$$j\sqrt{2}\bar{I}_{as} = I_{ds} + jI^r_{qs} \tag{6.4-8}$$

Substituting (6.4-1) and (6.4-2) into (6.4-6) and using (6.4-7) and (6.4-8) yields

$$\bar{V}_{as} = (r_s + j\omega_r L_q)\bar{I}_{as} + \bar{E}_a \tag{6.4-9}$$

where

$$\bar{E}_a = \frac{1}{\sqrt{2}}\left[\omega_r(L_d - L_q)I^r_{ds} + \omega_r\lambda'^r_m\right]e^{j0} \tag{6.4-10}$$

In Chapter 5 the phasor diagram for the synchronous machine was referenced to the phasor of v_{as} ($\bar{V}_{as}$), which was positioned along the real axis. Note that in the case of the synchronous machine the phase angle of $\bar{E}_a$ was δ [see (5.9-18)], whereas $\bar{E}_a$ for the brushless dc machine [see (6.4-10)] is along the reference (real) axis.

Common Operating Mode

From our earlier discussion we are aware that the values of V^r_{qs} and V^r_{ds} are determined by the firing of the driving inverter. However, the condition with $\phi_v = 0$, whereupon $V^r_{qs} = \sqrt{2}V_s$ and $V^r_{ds} = 0$, is used in most applications. In this case, (6.4-2) may be solved for I^r_{ds} in terms of I^r_{qs}.

$$I^r_{ds} = \frac{\omega_r L_q}{r_s} I^r_{qs} \qquad \text{for } \phi_v = 0 \tag{6.4-11}$$

Substituting (6.4-11) into (6.4-1) yields

$$V_{qs}^r = \left(\frac{r_s^2 + \omega_r^2 L_q L_d}{r_s}\right) I_{qs}^r + \omega_r \lambda_m^{\prime r} \qquad \text{for } \phi_v = 0 \tag{6.4-12}$$

We now start to see a similarity between the voltage equation for the brushless dc machine operated in this mode ($\phi_v = 0$) and the dc machine discussed in Chapter 2. From (2.3-1) the steady-state armature voltage equation of a dc shunt machine is

$$V_a = r_a I_a + \omega_r L_{AF} I_f \tag{6.4-13}$$

If we neglect $\omega_r^2 L_q L_d$ in (6.4-12) and if we assume the field current is constant in (6.4-13), then the two equations are identical in form. Let's note another similarity. If we neglect the inductances, or set $L_q = L_d$, then the expression for the torque given by (6.4-3) is identical in form to that of a dc shunt machine with a constant field current given by (2.3-5). We now see that the brushless dc motor is called a brushless dc motor, not because it has the same physical configuration as a dc machine but because its terminal characteristics may be made to resemble those of a dc machine. We must be careful, however, because in order for (6.4-12) and (6.4-13) to be identical in form, the term $\omega_r^2 L_q L_d$ must be significantly less than r_s. Let us see what effects this term has upon the torque versus speed characteristics. If we solve (6.4-12) for I_{qs}^r and we take that result along with (6.4-11) for I_{ds}^r and substitute these expressions into the expression for T_e (6.4-3) and if we assume that $L_q = L_d$, we obtain the following expression for torque:

$$T_e = \left(\frac{3}{2}\right)\left(\frac{P}{2}\right)\frac{r_s \lambda_m^{\prime r}}{r_s^2 + \omega_r^2 L_s^2}(V_{qs}^r - \omega_r \lambda_m^{\prime r}) \qquad \text{for } \phi_v = 0 \tag{6.4-14}$$

We have used L_s for L_q and L_d because we have assumed that $L_q = L_d$.

The steady-state, torque–speed characteristics for a typical brushless dc motor are shown in Fig. 6.4-1. Therein $L_{mq} = L_{md}$ and $\phi_v = 0$; hence, Fig. 6.4-1 is a plot of (6.4-14). If $\omega_r^2 L_s^2$ is neglected, then (6.4-14) yields a straight line T_e versus ω_r characteristic for a constant V_{qs}^r. Thus, if $\omega_r^2 L_s^2$ could be neglected, the plot shown in Fig. 6.4-1 would be a straight line. Although the T_e versus ω_r is approximately linear over the region of motor operation where $T_e \geq 0$ and $\omega_r \geq 0$, it is not linear over the complete speed range. In fact, we see from Fig. 6.4-1 that there appears to be a maximum and minimum torque. Let us take the derivative of (6.4-14) with respect to ω_r and set the result to zero and solve for ω_r. Thus, zero slope of the torque versus speed characteristics for $L_q = L_d = L_s$, $V_{qs}^r = \sqrt{2}V_s$, and $V_{ds}^r = 0$ ($\phi_v = 0$) occurs at

$$\omega_{rMT} = \frac{V_{qs}^r}{\lambda_m^{\prime r}} \pm \sqrt{\left(\frac{V_{qs}^r}{\lambda_m^{\prime r}}\right)^2 + \left(\frac{r_s}{L_s}\right)^2} \qquad \text{for } \phi_v = 0 \tag{6.4-15}$$

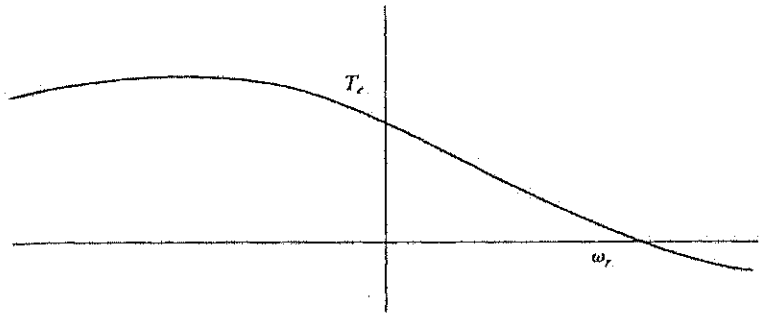

Figure 6.4-1 Torque-speed characteristics of a brushless dc motor with $L_{mq} = L_{md}$ ($L_q = L_d$), $\phi_v = 0$, $V_{qs}^r = \sqrt{2}V_s$, and $V_{ds}^r = 0$.

Due to the high reluctance of the magnetic material in the d axis, L_d is less than L_q for some machine designs. In most cases, whether $L_q > L_d$ or $L_q < L_d$, saliency has only secondary effects upon the torque–speed characteristics over the region of interest ($T_e \geq 0$ and $\omega_r \geq 0$). This is shown in Fig. 6.4-2 where $L_{mq} = 0.6L_{md}$ for the machine considered in Fig. 6.4-1.

Operating Modes Achievable by Phase Shifting the Applied Voltages

Let us return to (6.4-1)–(6.4-3), and this time we will not restrict ϕ_v to zero. Hence, from (6.4-2) we have

$$I_{ds}^r = \frac{V_{ds}^r + \omega_r L_q I_{qs}^r}{r_s} \tag{6.4-16}$$

Substituting into (6.4-1) yields

$$V_{qs}^r = \frac{r_s^2 + \omega_r^2 L_q L_d}{r_s} I_{qs}^r + \frac{\omega_r L_d}{r_s} V_{ds}^r + \omega_r \lambda_m'^r \tag{6.4-17}$$

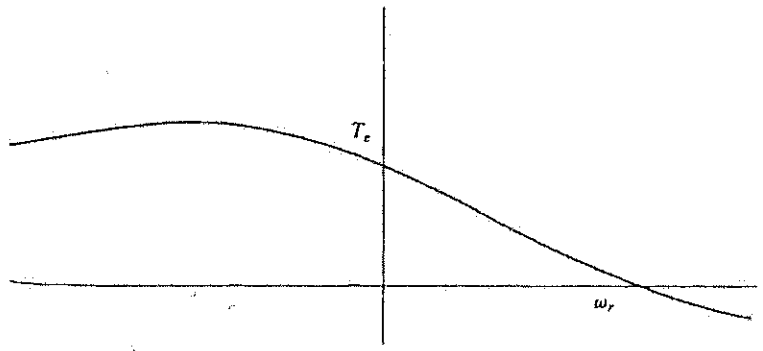

Figure 6.4-2 Same as Fig. 6.4-1 with $L_{mq} = 0.6L_{md}$.

Let us again set $L_q = L_d = L_s$, which simplifies our work. In this case, T_e and i'_{qs} differ only by a constant multiplier. Solving (6.4-14) for I'_{qs} yields

$$I'_{qs} = \frac{r_s}{r_s^2 + \omega_r^2 L_s^2}\left(V'_{qs} - \frac{L_s}{r_s} V'_{ds}\omega_r - \lambda'^{r}_{m}\omega_r\right) \tag{6.4-18}$$

We see from (6.3-20) and (6.3-21) that if we consider only the fundamental component of the 3-phase applied stator voltages, then we have

$$V'_{qs} = \sqrt{2}V_s \cos\phi_v \tag{6.4-19}$$

$$V'_{ds} = -\sqrt{2}V_s \sin\phi_v \tag{6.4-20}$$

wherein ϕ_v is determined by the switching of the inverter. Substituting (6.4-19) and (6.4-20) into (6.4-18) yields

$$I'_{qs} = \frac{\sqrt{2}r_s V_s}{r_s^2 + \omega_r^2 L_s^2}[\cos\phi_v + (\tau_s \sin\phi_v - \tau_v)\omega_r] \tag{6.4-21}$$

Here we are using time constants, or what appear to be time constants, in a steady-state equation. This is not normally done; however, it allows us to work more efficiently. The constant τ_s is L_s/r_s. It is the electrical or stator time constant which is analogous to the armature circuit time constant, τ_a, of a dc machine. The quantity τ_v is defined here as

$$\tau_v = \frac{\lambda'^{r}_{m}}{\sqrt{2}V_s} \tag{6.4-22}$$

It is introduced for our convenience. Be careful, however. Although τ_v has the unit of seconds, it is not a constant; it will change with V_s. In speed control systems the inverter supplying the brushless dc motor may provide a means to change the magnitude of V_s.

Equation (6.4-21) is an expression for I'_{qs}, and thus T_e, in terms of the angle ϕ_v which is the phase shift of the fundamental component of the voltage v_{as} ahead of the q axis of the rotor. There are several pieces of information that can be gained from this equation. First let us find the maximum and minimum with respect to ϕ_v. This of course may be accomplished by taking the derivative of (6.4-21) with respect to ϕ_v and setting the result equal to zero. This yields

$$0 = -\sin\phi_v + \tau_s\omega_r\cos\phi_v \tag{6.4-23}$$

which says that at a given rotor speed a maximum or minimum value of $I'_{qs}(T_e)$ occurs when

$$\phi_{vMT} = \tan^{-1}(\tau_s\omega_r) \tag{6.4-24}$$

Hence, the maximum or minimum steady-state electromagnetic torque, with ϕ_{vMT} given by (6.4-24), may be determined by substituting (6.4-24) into (6.4-21) and then

substituting the results into (6.3-14) with $L_q = L_d = L_s$. Thus, the maximum or minimum steady electromagnetic torque for a given rotor speed may be expressed as

$$T_{eM} = \left(\frac{3}{2}\right)\left(\frac{P}{2}\right)\frac{\sqrt{2}V_s r_s \lambda_m'^r}{r_s^2 + \omega_r^2 L_s^2}\left[\frac{(r_s^2 + \omega_r^2 L_s^2)^{1/2}}{r_s} - \frac{\lambda_m'^r \omega_r}{\sqrt{2}V_s}\right] \tag{6.4-25}$$

which may also be written as

$$T_{eM} = \left(\frac{3}{2}\right)\left(\frac{P}{2}\right)\frac{\sqrt{2}V_s^2 \tau_v}{r_s(1 + \tau_s^2\omega_r^2)}[(1 + \tau_s^2\omega_r^2)^{1/2} - \tau_v\omega_r] \tag{6.4-26}$$

Although (6.4-24)–(6.4-26) are valid for any speed, we are generally concerned with positive values of ω_r and T_e for steady-state operation. With this in mind, let us look back to (6.4-21) and assume that the speed is positive. With this assumption, T_e is positive if

$$\cos\phi_v + \tau_s\omega_r \sin\phi_v > \tau_v\omega_r \tag{6.4-27}$$

Let us assume that ϕ_v is $\pi/2$, which means that $V_{qs}^r = 0$ and $V_{ds}^r = -\sqrt{2}V_s$. With $\phi_v = \pi/2$, (6.4-27) becomes

$$\tau_s > \tau_v \tag{6.4-28}$$

Equation (6.4-28) tells us that if $\phi_v = \pi/2$ and if $\tau_s > \tau_v$, the torque will always be positive for $\omega_r > 0$. It follows that if $\phi_v = \pi/2$ and if $\tau_s = \tau_v$, the torque will be zero regardless of the speed of the rotor or if $\tau_s < \tau_v$ the torque will be negative for $\omega_r > 0$.

We will derive one more relationship from (6.4-21). For a fixed value of ϕ_v, the speeds at which the maximum and minimum torques occur may be determined by taking the derivative of (6.4-21) with respect to ω_r and setting the result to zero. This yields

$$\omega_{rMT} = \frac{1}{\tau_s \sin\phi_v - \tau_v}\left[-\cos\phi_v \pm \frac{1}{\tau_s}\sqrt{\tau_s^2 + \tau_v^2 - 2\tau_s\tau_v\sin\phi_v}\right] \tag{6.4-29}$$

It is left to the reader to show that (6.4-29), with $\phi_v = 0$, is (6.4-15).

The steady-state, torque–speed characteristics for a brushless dc machine are shown in Fig. 6.4-3 for $L_q = L_d$ and for $L_{mq} = 0.6L_{md}$ in Fig. 6.4-4. In order to illustrate the limits of the torque–speed characteristics for the various possible values of ϕ_v, plots of torque are shown for $\phi_v = 0$, $\pm\pi/2$, π, and ϕ_{vMT}. The maximum torque for $\omega_r > 0$ is also plotted in Fig. 6.4-3. The machine parameters for the characteristics shown in Fig. 6.4-3 are $r_s = 3.4\,\Omega$, $L_{ls} = 1.1$ mH, and $L_{mq} = L_{md} = 11$ mH; thus $L_q = L_d = L_s = 12.1$ mH. The device is a 4-pole machine; and when it is driven at 1000 r/min, the open-circuit winding-to-winding voltage is sinusoidal

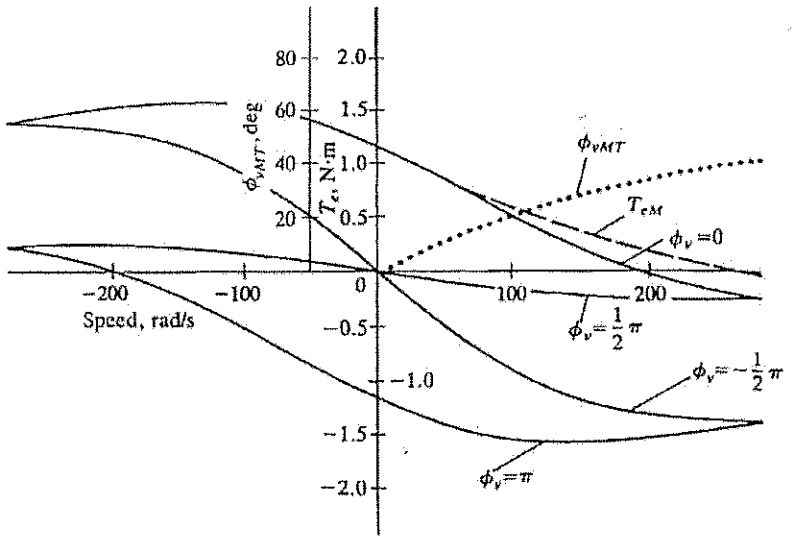

Figure 6.4-3 Torque–speed characteristics of a brushless dc machine with $L_{mq} = L_{md} (L_q = L_d)$.

with a peak-to-peak value of 60 V. From this, λ_m^{fr} is calculated to be 0.0827 V·s. (The reader should verify this calculation.) The value of V_s is 11.25 V.

We see that this machine, which is commercially available, yields negative T_e for $\phi_v = \pi/2$ for $\omega_r > 0$. Therefore $\tau_s < \tau_v$. Let us see: $\tau_s = (12.1 \times 10^{-3})/3.4 = 3.56$ ms; $\tau_v = 0.0827/(\sqrt{2} \times 11.25) = 5.2$ ms. In references 3 and 4 it was

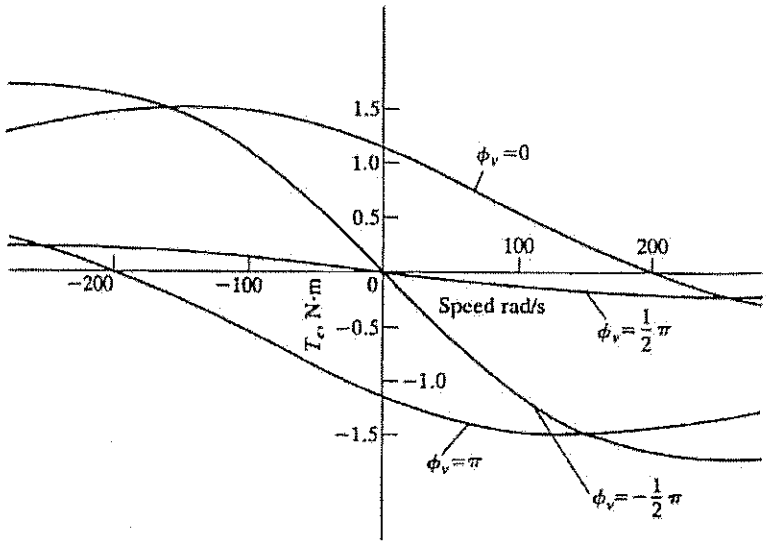

Figure 6.4-4 Torque–speed characteristics of a brushless dc machine with $L_{mq} = 0.6 L_{md}$.

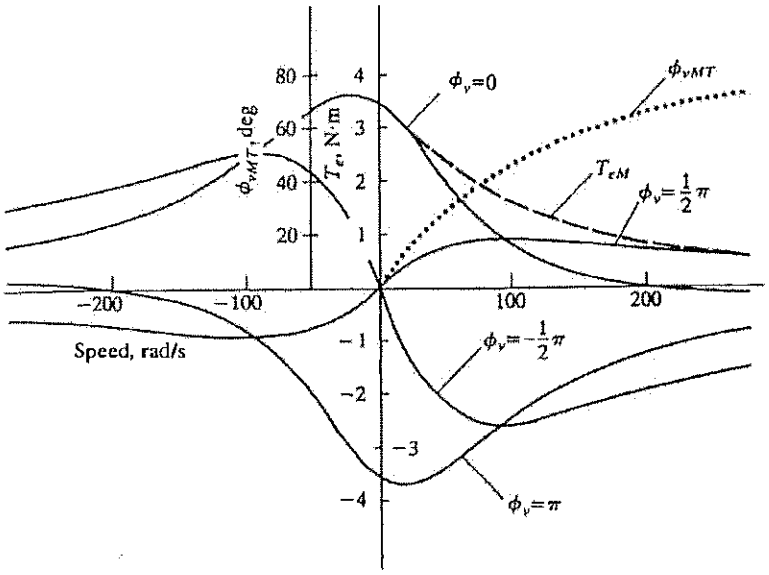

Figure 6.4-5 Torque–speed characteristics of a brushless dc motor with τ_s increased by a factor of three by decreasing r_s.

experimentally verified that advancing ϕ_v from zero, increased the torque at rotor speeds greater than zero. Therein, it is suggested that this might be a means of increasing the torque at high speeds. The parameters of the machine used in reference 4 are given and $\tau_s > \tau_v$. We now understand why. The influence of τ_s upon the steady-state torque–speed characteristics is illustrated by Figs. 6.4-5 and 6.4-6. In

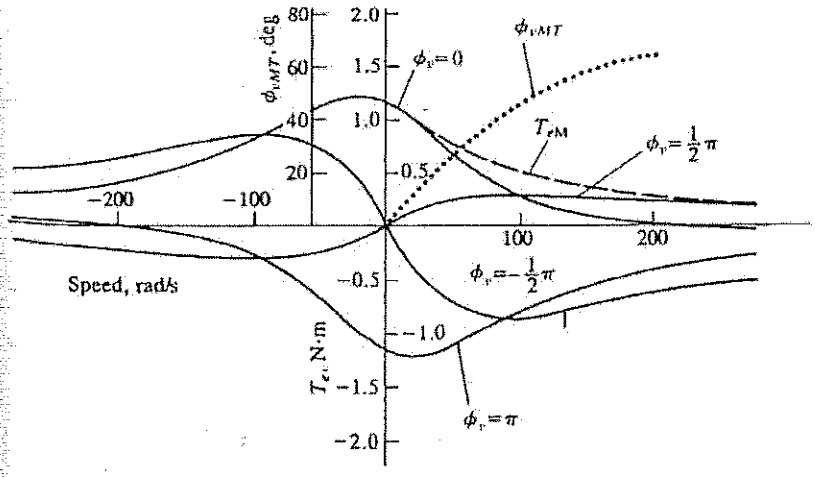

Figure 6.4-6 Torque–speed characteristics of a brushless dc motor with τ_s increased by a factor of three by increasing L_{ss}.

Fig. 6.4-5, τ_s is increased by a factor of 3 ($\tau_s = 3 \times 3.56$ ms) by decreasing r_s. In Fig. 6.4-6, τ_s is increased by a factor of 3 by increasing L_s.

6.5 DYNAMIC PERFORMANCE

It is instructive to observe the machine variables during free acceleration and step changes in load torque with $\phi_v = 0$. The machine parameters are those given previously with $J = 1 \times 10^{-4}$ kg·m^2. In this section the dynamic performance is shown, by computer traces, for applied stator phase voltages that are sinusoidal

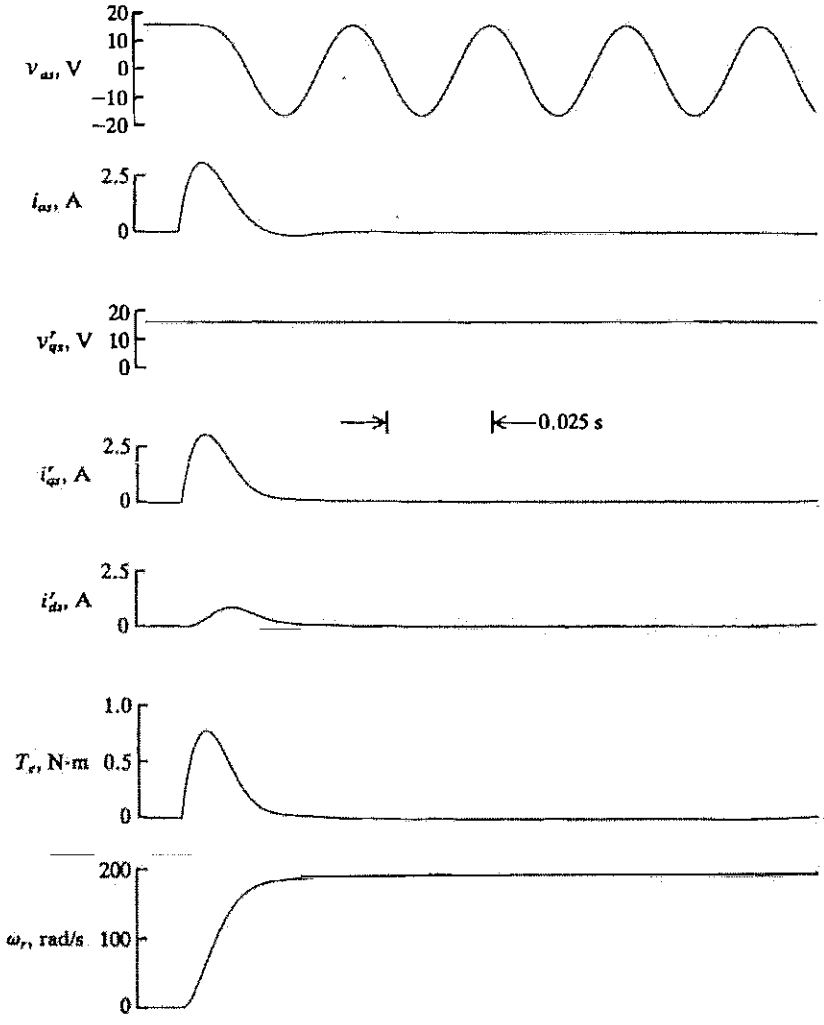

Figure 6.5-1 Free acceleration characteristics of a brushless dc motor ($\phi_v = 0$).

and that are stepped as would be the case if a typical six-step voltage source inverter were used to supply the machine [5–7]. Although it may seem inappropriate because we have yet to discuss the operation of the inverter, it does provide a first look at the machine variables in a drive application, and most important it provides a justification of the sinusoidal approximation of the actual six-step phase voltages. The brushless dc motor-inverter drives are considered in detail in Chapter 15.

Sinusoidal Phase Voltages

The free acceleration characteristics with sinusoidal phase voltages are shown in Fig. 6.5-1. The applied stator phase voltages are of the form given by (6.3-16)–(6.3-18) with $v_s = 11.25$ V. The phase voltage v_{as}, phase current i_{as}, q-axis voltage v'_{qs}, q-axis current i'_{qs}, d-axis current i'_{ds}, electromagnetic torque T_e, and rotor speed ω_r in electrical rad/s are plotted in Fig. 6.5-1. It is clear that because $\phi_v = 0$, we have $v'_{ds} = 0$. The device is a 4-pole machine; thus 200 electrical rad/s is 955 r/min. A plot of T_e versus ω_r is shown in Fig. 6.5-2 for the free acceleration depicted in Fig. 6.5-1. The steady-state, torque–speed characteristic is superimposed for purposes of comparison.

In Fig. 6.5-1, the rapid acceleration of the brushless dc motor is apparent. In fact the rotor reaches full speed in less than 0.05 s. The acceleration is so rapid that it is difficult to observe the change in frequency of v_{as} as the motor accelerates from stall. In order to illustrate the frequency change during the acceleration period, the free acceleration characteristics given in Figs. 6.5-3 and 6.5-4 are for an inertia of five times the inertia of the rotor (5×10^{-4} kg·m^2). It is important to note that the dynamic torque–speed characteristics shown in Figs 6.5-2 and 6.5-4 differ from the steady-state, torque–speed characteristics. One must be aware of

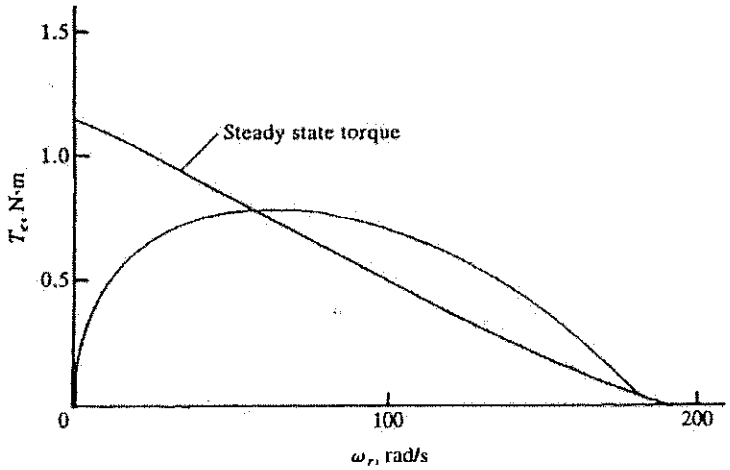

Figure 6.5-2 Torque–speed characteristics for free acceleration shown in Fig. 6.5-1.

this discrepancy, if one chooses to use the expression for the steady-state torque in a transfer function formulation describing the dynamic characteristics of a brushless dc motor.

The performance during step changes in load torque is illustrated in Fig. 6.5-5. Initially the machine is operating with $T_L = 0.1$ N·m. The load torque is suddenly stepped to 0.4 N·m. The machine slows down and once steady-state operation is

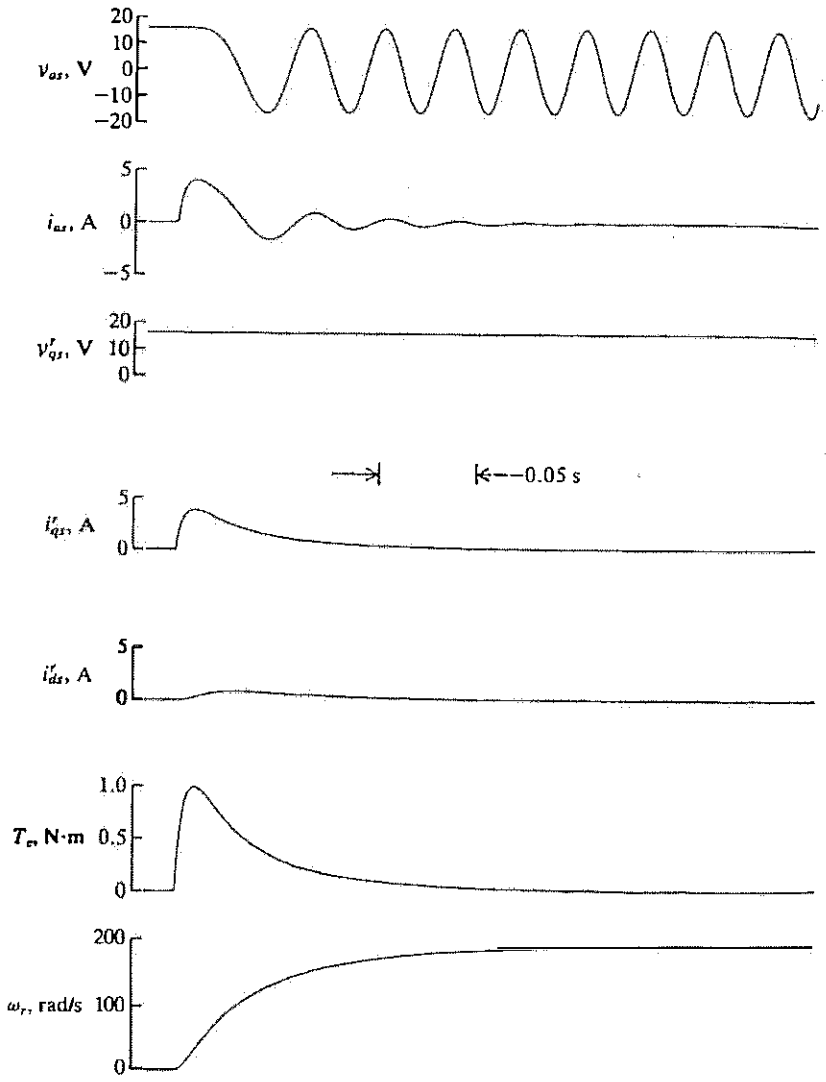

Figure 6.5-3 Free acceleration characteristics of a brushless dc motor ($\phi_v = 0$) with inertia equal to five times rotor inertia.

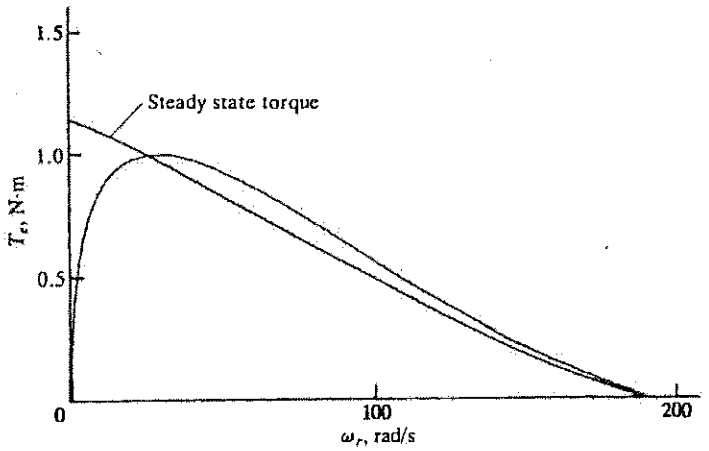

Figure 6.5-4 Torque–speed characteristics for free acceleration shown in Fig. 6.5-3.

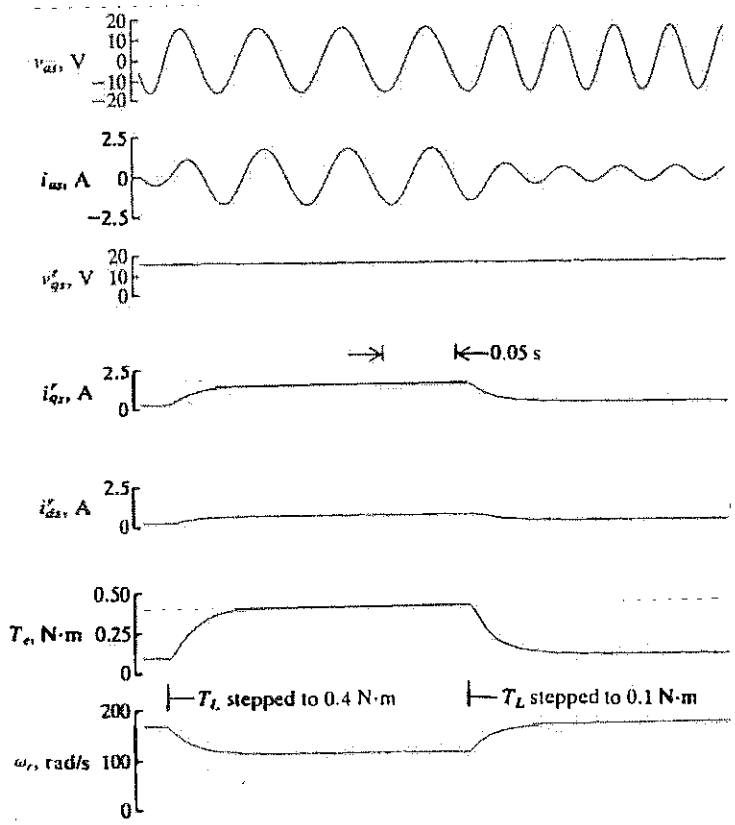

Figure 6.5-5 Dynamic performance of a brushless dc motor ($\phi_r = 0$) during step changes in load torque. Total inertia is twice rotor inertia.

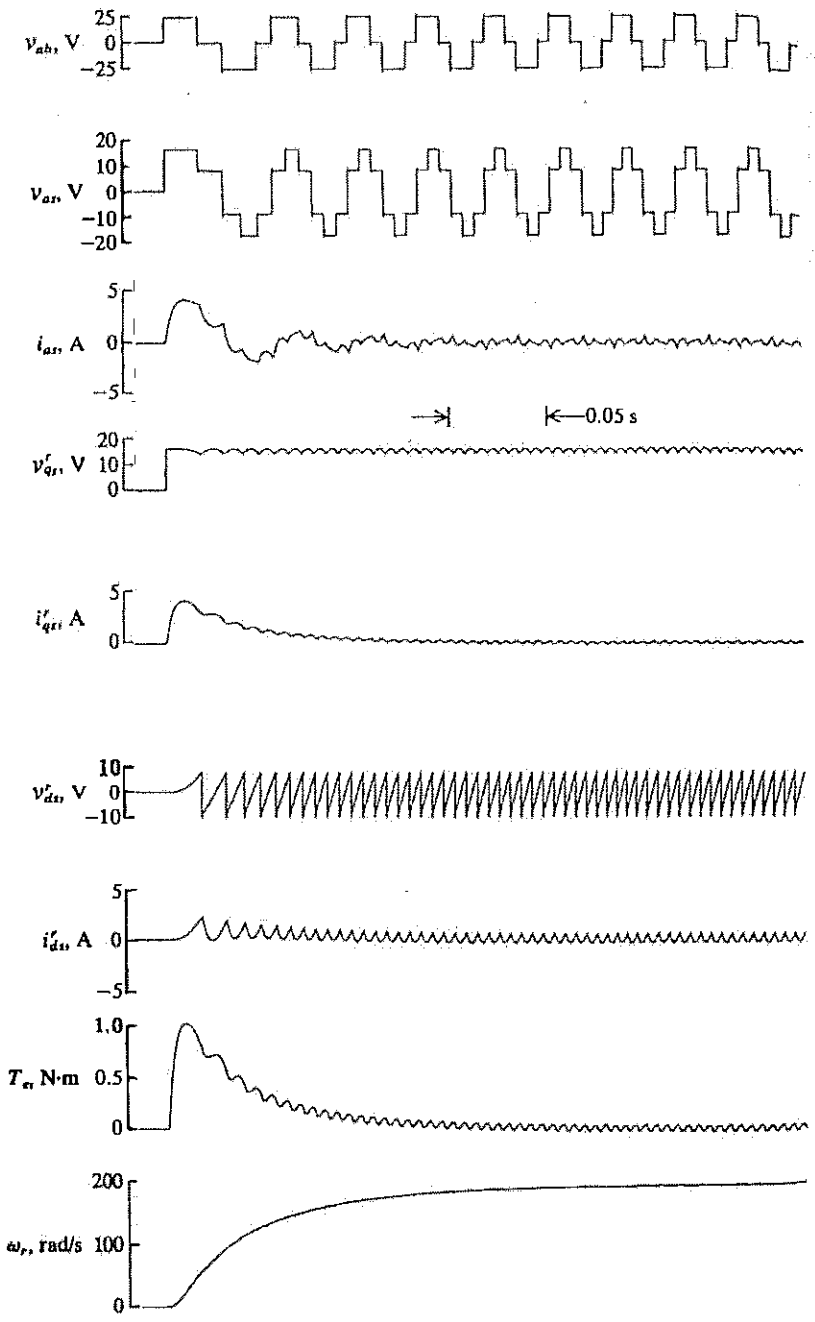

Figure 6.5-6 Free acceleration characteristics of a brushless dc motor supplied from a voltage source inverter ($\phi_v = 0$). Total inertia is five times rotor inertia. Compare with Fig. 6.5-3.

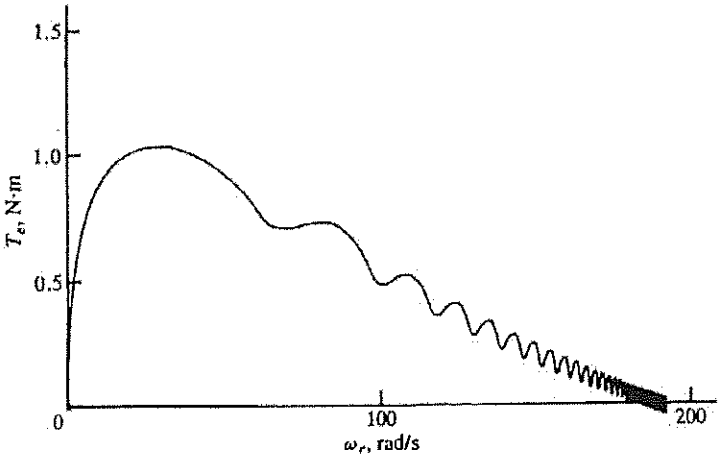

Figure 6.5-7 Torque–speed characteristics for free acceleration shown in Fig. 6.5-6.

established, the load torque is stepped back to 0.1 N · m. In these studies, the inertia is 2×10^{-4} kg·m^2, which is twice the inertia of the rotor.

Six-Step Phase Voltages

The free acceleration characteristics with the machine supplied from a typical voltage source inverter are shown in Fig. 6.5-6. The voltage v'_{ds} is plotted in addition to the variables shown in Fig. 6.5-3. It is recalled that with the sinusoidal approximation, v'_{ds} is zero for $\phi_v = 0$. We see in Fig. 6.5-6 that the average value of v'_{ds} is zero. The torque versus speed characteristics for this free acceleration are shown in Fig. 6.5-7.

In order to compare with the sinusoidal approximation, the inverter voltage was selected so that the constant component of v'_{qs} is equal to the value used in the case of ac applied stator voltages. It is interesting to note that during the initial acceleration period, in Fig. 6.5-6, before the first step (switching) occurs in v_{as}, the torque is larger than with ac voltages applied (Fig. 6.5-3). This is due to the fact that a constant voltage is applied to the phases until the first switching occurs, and this constant voltage is larger than the effective value of the ac voltage during the same interval.

The dynamic performance during load torque switching is shown in Fig. 6.5-8. As in Fig. 6.5-5 the inertia is twice the rotor inertia (2×10^{-4} kg · m^2) and the load torque is switched from 0.1 N · m to 0.4 N · m and then back to 0. IN · m. It is apparent that the sinusoidal approximation of the phase voltages is quite accurate in portraying dynamic and steady-state operation of a brushless dc motor supplied from a typical voltage source inverter. We will find that this fact is very useful for control design purposes because it justifies the neglecting of the harmonics due to the switching of the inverters.

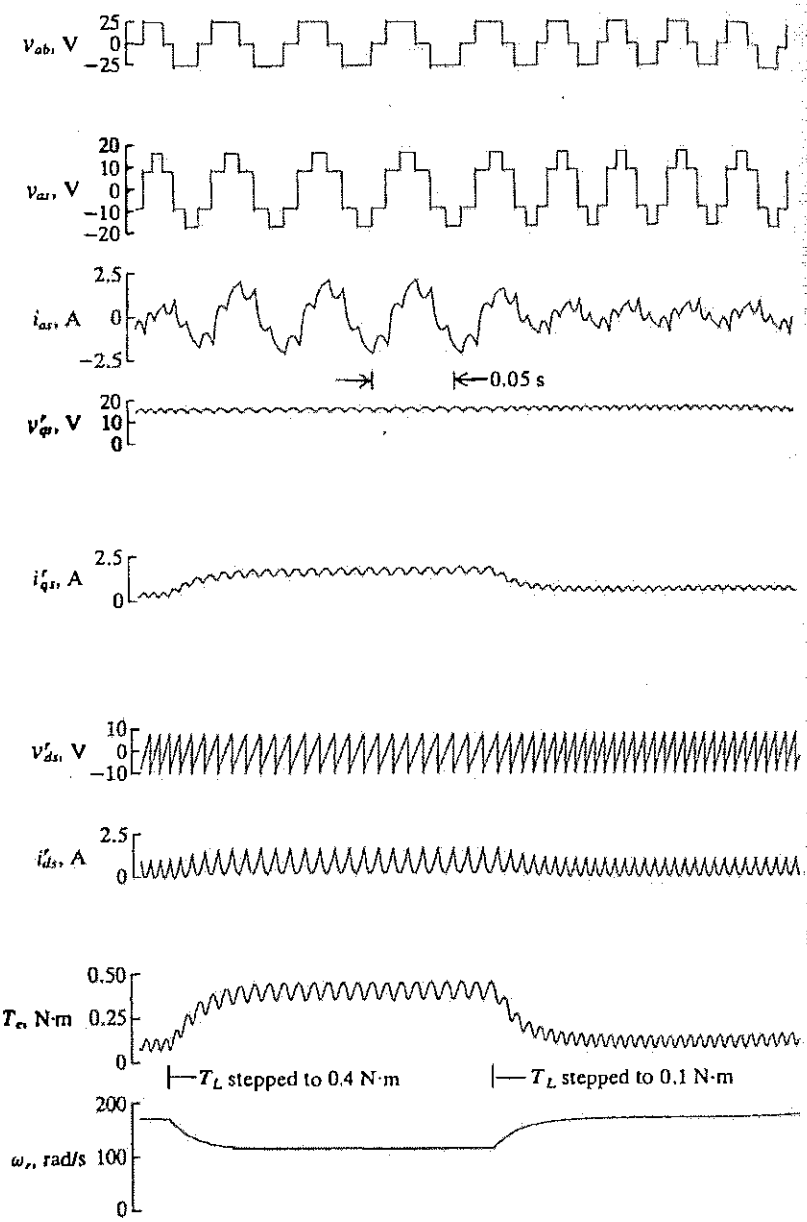

Figure 6.5-8 Dynamic performance during step changes in load torque of a brushless dc motor supplied from a voltage source inverter ($\phi_v = 0$). Total inertia is twice rotor inertia. Compare with Fig. 6.5-5.

Chapter 15

BRUSHLESS dc MOTOR DRIVES

15.1 INTRODUCTION

For the purposes of this text, a brushless dc motor drive is defined as a permanent-magnet synchronous machine used in the context of a drive system with rotor position feedback. There are a great variety of brushless dc motor drives. Generally, these drives may be described by the block diagram in Fig. 15.1-1. Therein, the brushless dc drive is seen to consist of four main parts: a power converter, a permanent-magnet synchronous machine (PMSM), sensors, and a control algorithm. The power converter transforms power from the source (such as the local utility or a dc supply bus) to the proper form to drive the permanent-magnet synchronous machine, which, in turn, converts electrical energy to mechanical energy. One of the salient features of the brushless dc drive is the rotor-position sensor (or at least an observer). Based on the rotor position and a command signal(s), which may be a torque command, voltage command, speed command, and so on, the control algorithms determine the gate signal to each semiconductor in the power electronic converter.

The structure of the control algorithms determines the type of brushless dc drive, of which there are two main classes: voltage-source-based drives and current-source (or regulated) drives. Both voltage- and current-source-based drives may be used with permanent-magnet synchronous machines with either sinusoidal or nonsinusoidal back emf waveforms. Machines with sinusoidal back emfs may be controlled so as to achieve nearly constant torque; however, machines with a nonsinusoidal back emf offer reduced inverter sizes and reduced losses for the same power level. The discussion in this chapter will focus on the machines with sinusoidal back emfs; for information on the nonsinusoidal drives, the reader is referred to references 1–3.

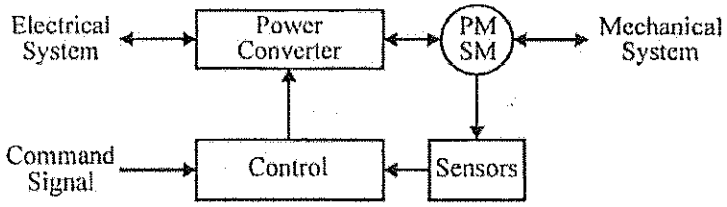

Figure 15.1-1 Brushless dc drive.

In this chapter, a variety of voltage- and current-source-based drives featuring machines with sinusoidal back emf waveforms are analyzed. For each drive considered, detailed simulations will be used to demonstrate performance. Next, average-value models for each drive are set forth, along with a corresponding linearized model for control synthesis. Using these models, the steady-state, harmonic, transient, and dynamic performance of each drive considered will be set forth. Extended design examples will be used to illustrate the performance of the drive within the context of a control system environment.

15.2 VOLTAGE-SOURCE INVERTER DRIVES

Figure 15.2-1 illustrates a voltage-source inverter-based brushless dc drive. Power is supplied from the utility through a transformer, which is depicted as an equivalent voltage behind inductance. The transformer output is rectified, and the rectifier output is connected to the dc link filter, which may be simply an LC filter (L_{dc}, C_{dc}) but which may include a stabilizing filter (L_{st}, r_{st}, C_{st}) as well. The filtered rectifier output is used as a dc voltage source for the inverter, which drives the permanent-magnet synchronous machine. As can be seen, rotor position is an input to the controller. Based upon rotor position and other inputs, the controller determines the switching states of each of the inverter semiconductors. The command signal to the controller may be quite varied depending upon the structure of the controls in the system in which the drive is embedded; it will often be a torque command. Other inputs to the control algorithms may include rotor speed, dc link voltage, and rectifier voltage. Other outputs may include gate signals to the rectifier thyristors if the rectifier is phase-controlled.

Variables of particular interest in Fig. 15.2-1 include the utility supply voltages, v_{au}, v_{bu}, and v_{cu}, the utility currents into the rectifier, i_{au}, i_{bu}, and i_{cu}, the rectifier output voltage, v_r, the rectifier current, i_r, the stabilizing filter current, i_{st}, the stabilizing filter capacitor voltage, v_{st}, the inverter voltage, v_{dc}, the inverter current, i_{dc}, the three-phase currents into the machine, i_{as}, i_{bs}, and i_{cs}, the machine line-to-neutral voltages, v_{as}, v_{bs}, and v_{cs}, and the electrical rotor position, θ_r.

Even within the context of the basic system shown in Fig. 15.2-1, there are many possibilities for control, depending upon whether or not the rectifier is phase-controlled and the details of the inverter modulation strategy. Regardless of the

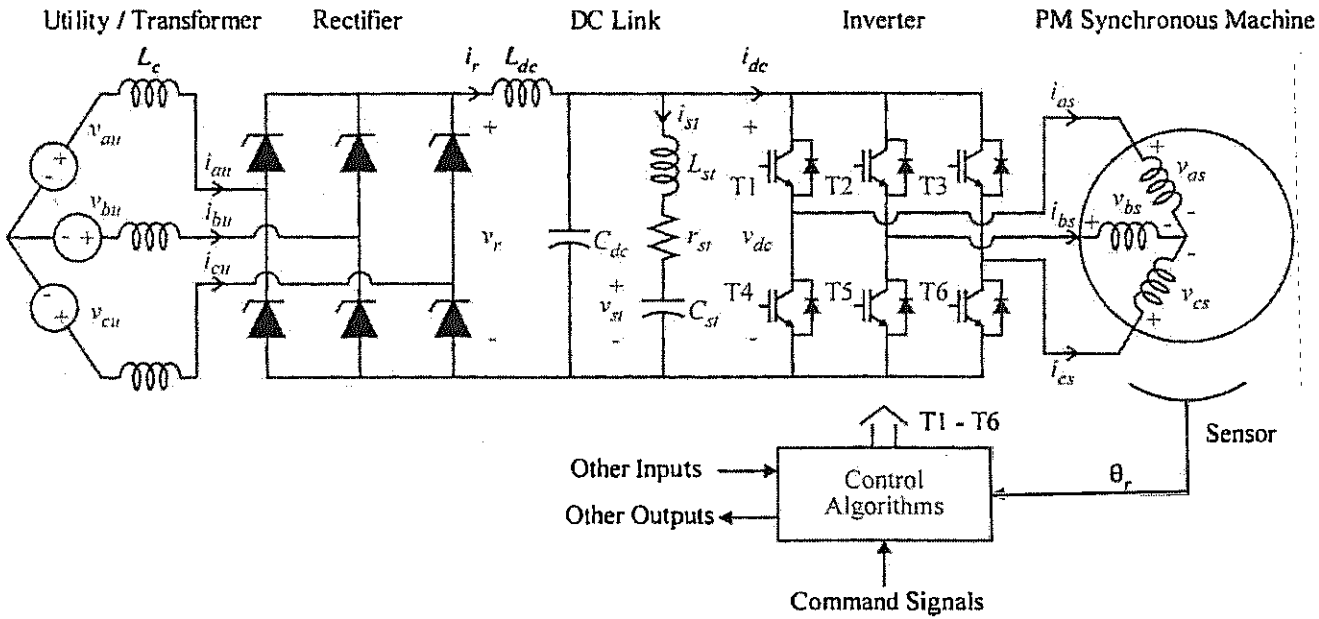

Figure 15.2-1 Voltage-source inverter-fed brushless dc motor drive.

559

control strategy, it is possible to relate the operation of the converter back to the idealized analysis set forth in Chapter 6, which will be the starting point for our investigation into voltage-source inverter-fed brushless dc drive systems.

15.3 EQUIVALENCE OF VSI SCHEMES TO IDEALIZED SOURCE

In order to make use of the idealized analysis of voltage-source operation of the brushless de machine set forth in Chapter 6, it is necessary to relate the voltage-source inverter to an ideal source. This relationship is a function of the type of modulation strategy used. In this section, the equivalencies of 180° voltage-source operation, duty-cycle modulation, sine-triangle modulation, third-harmonic injection modulation, and space-vector modulation strategies to idealized sources are established.

The 180° voltage-source inverter-based brushless de drive is the simplest of all the topologies to be considered in terms of generating the signals required to control the inverter. It is based on the use of relatively inexpensive Hall-effect rotor position sensors. For this reason, the 180° voltage-source inverter drive is a relatively low-cost drive. Furthermore, because the frequency of the switching of the semiconductors corresponds to the speed of the machine, fast semiconductor switching is not important, and switching losses will therefore be negligible. However, the inverter does produce considerable harmonic content that will result in increased machine losses.

In the 180° voltage-source inverter drive, the on or off status of each of the semiconductors is directly tied to electrical rotor position, which is accomplished through the use of the Hall-effect sensors. These sensors can be configured to have a logical high output when they are under a south magnetic pole and a logic zero when they are under a north magnetic pole of the permanent magnet, and they are arranged on the stator of the brushless dc machine as illustrated in Fig. 15.3-1, where ϕ_h denotes

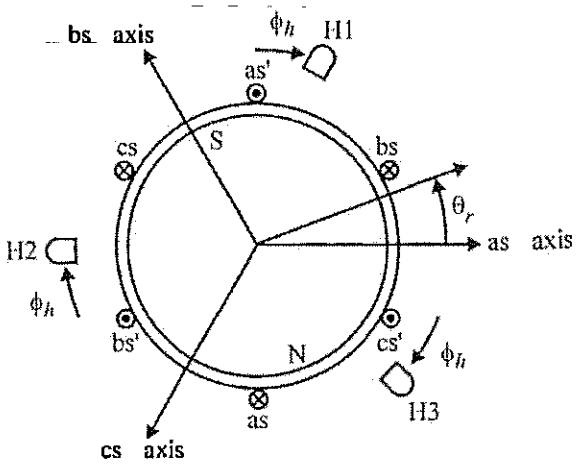

Figure 15.3-1 Electrical diagram of a brushless dc machine.

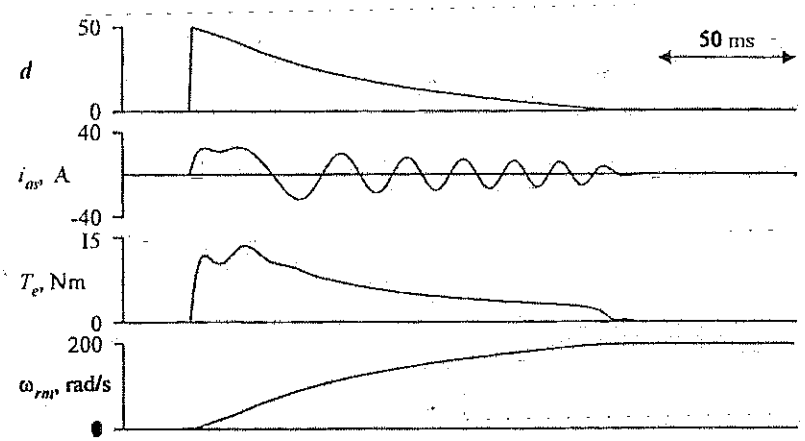

Figure 15.8-5 Start-up response of the closed-loop brushless dc drive.

applied voltage was effectively much lower than expected, the bandwidth for this large disturbance is not nearly the 100 Hz indicated in Fig. 15.8-4. Finally, the rated current for the machine is only 2.6 A, rms. Although the machine could probably withstand the temporary overcurrent, the inverter probably could not, and thus either the bandwidth should be reduced so as to alleviate the overcurrent or the duty cycle should be limited as a function of the current. Finally, close inspection reveals that at the end of the study, the speed is not 200 rad/s and does not even appear to be rapidly increasing. This is because the bandwidth of the compensation was chosen to be quite low, and as a result a small error in rotor speed will persist for some time, although it will eventually go to zero. A second design iteration addressing these issues is left to the reader as an exercise.

15.9 CURRENT-REGULATED INVERTER DRIVES

Sections 15.1–15.8 explored the performance of drives in which the machine is controlled through suitable regulation of the applied voltages. In the remainder of this chapter an alternate strategy is considered: control of the machine through the regulation of the stator currents. The hardware configuration for current-regulated inverter drives is identical to that of voltage-source inverter drives, as illustrated in Fig. 15.2-1. The only difference is in the way in which the gate signals to the individual semiconductors are established.

Current-regulated inverters have several distinctive features. First, because torque is a function of the machine current, the torque may be controlled with the same bandwidth by which the stator currents are controlled. In fact, it is often the case that for practical purposes the torque control is essentially instantaneous. A second feature of current-regulated drives is robustness with regard to changes in machine parameters. For example, current-regulated inverter drives are insensitive to

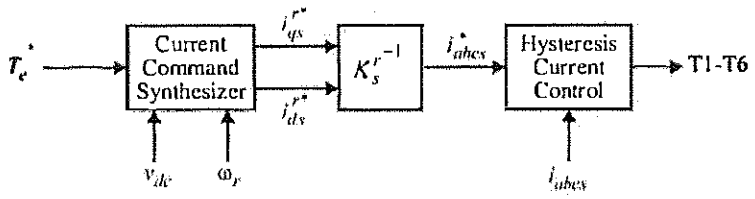

Figure 15.9-1 Hysteresis current-regulated drive.

parameter variations in the stator leakage inductance or stator resistance. Current-regulated drives are also robust in regard to faults. In the event of a winding-to-winding short circuit within the machine the currents are automatically limited, which prevents damage to the inverter. The currents are also automatically limited during start-up.

Figure 15.9-1 illustrates the control of the current-regulated drive. Therein, the q- and d-axis current commands, i_{qs}^{r*} and i_{ds}^{r*}, are formulated based on the commanded torque, T_e^*, electrical rotor speed, ω_r, and the inverter voltage, v_{dc}. Using the inverse transformation, the corresponding abc variable current command i_{abcs}^* is determined. Finally, based on the abc variable current command and the actual currents, the on and off status of each of the inverter semiconductors (T1–T6) is determined using the hysteresis current control strategy set forth in Section 13.8. An immediate question that arises is how the q- and d-axis current commands are generated to begin with; this question is addressed in detail in a following section. For the present it suffices to say that the command is determined in such a way that if the commanded currents are obtained, the commanded torque will also be obtained.

Figure 15.9-2 illustrates the steady-state performance of a hysteresis current-regulated brushless dc motor drive. Therein, the operating conditions are identical to those portrayed in Fig. 15.3-5 except for the modulation strategy. The q- and d-axis current commands are set to 1.73 A and 2.64 A, respectively, so that the fundamental component of the commanded current is identical to that in Fig. 15.3-5. As can be seen, although the modulation strategies are different, the waveforms produced by the sine-triangle modulation strategies and the hysteresis current strategy are very similar.

A second method to implement a current-regulated inverter drive is to utilize a current-control loop on a voltage-source inverter drive. This is illustrated in Fig. 15.9-3. Therein, the current command synthesizer serves the same function as in Fig. 15.9-1. Based on the commanded q- and d-axis currents and the measured q- and d-axis currents (determined by transforming the measured abc variable currents), the q- and d-axis voltage commands (v_{qs}^{r*} and v_{ds}^{r*}) are determined. The q- and d-axis voltage command is then converted to an abc variable voltage command v_{abcs}^* which is scaled in order to determine the instantaneous duty cycles, d_a, d_b, and d_c of the sine-triangle modulation strategy. Based on these duty cycles, T1–T6 are determined as described in Section 13.5. There are several methods of developing the current control, such as a synchronous current regulator [7]. An example of the design of a feedback linearization-based controller is considered in Example 15B.

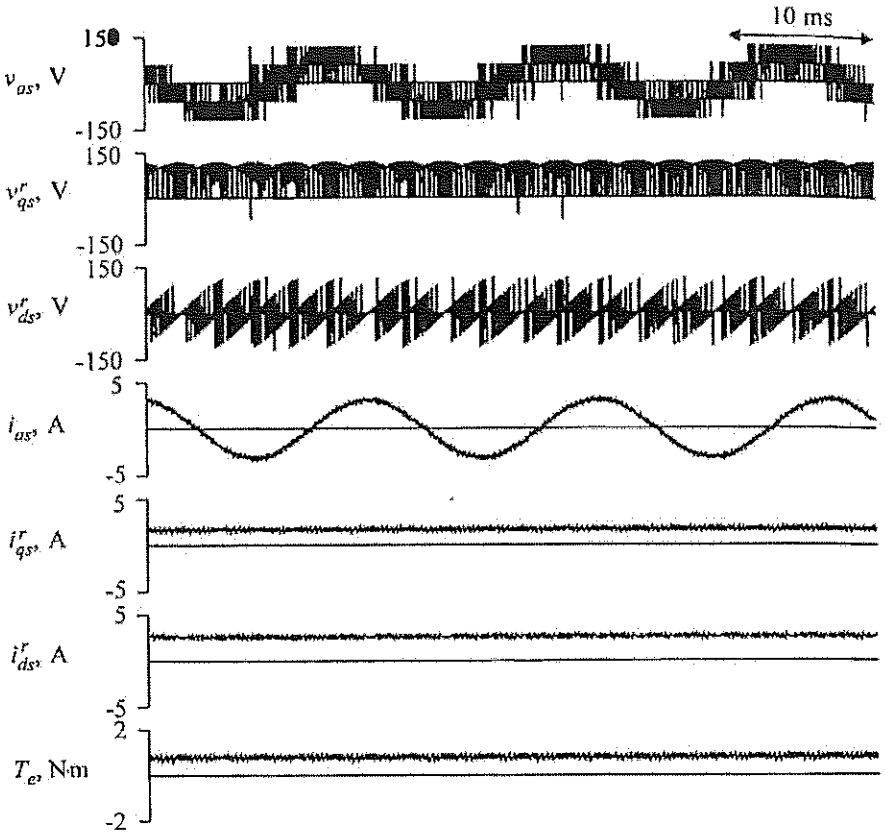

Figure 15.9-2 Steady-state performance of a hysteresis-modulated brushless dc motor drive.

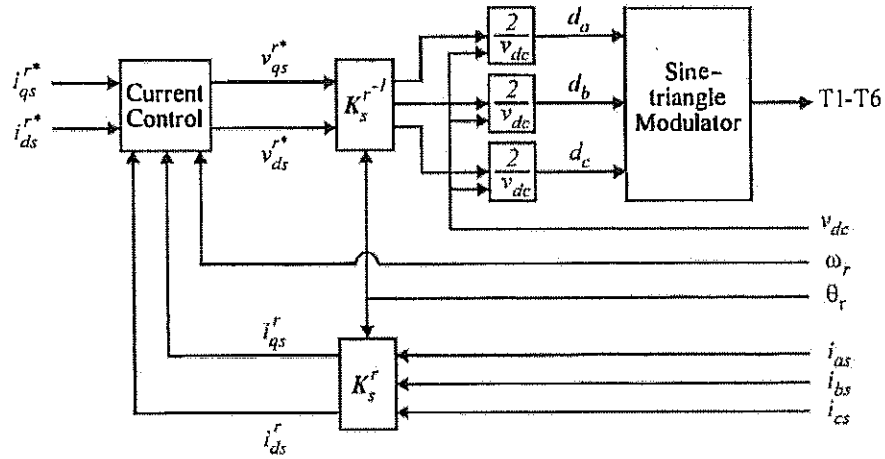

Figure 15.9-3 A sine-triangle-based current regulator.

Example 15B. Let us consider the design of a current regulator for a nonsalient brushless dc motor. The goal is to determine the q- and d-axis voltage command so that the actual currents become equal to the commanded currents. Let us attempt to accomplish this goal by specifying the voltage commands as

$$v_{qs}^{r*} = \omega_r(L_{ss}i_{ds}^r + \lambda_m^r) + \left(K_p + \frac{K_i}{s}\right)(i_{qs}^{r*} - i_{qs}^r) \tag{15B-1}$$

$$v_{ds}^{r*} = -\omega_r L_{ss} i_{qs}^r + \left(K_p + \frac{K_i}{s}\right)(i_{ds}^{r*} - i_{ds}^r) \tag{15B-2}$$

where s denotes the Laplace operator, K_p is the proportional gain, and K_i is the integral gain. This control algorithm contains feedback terms that cancel the nonlinearities in the stator voltage equations, feedforward terms that cancel

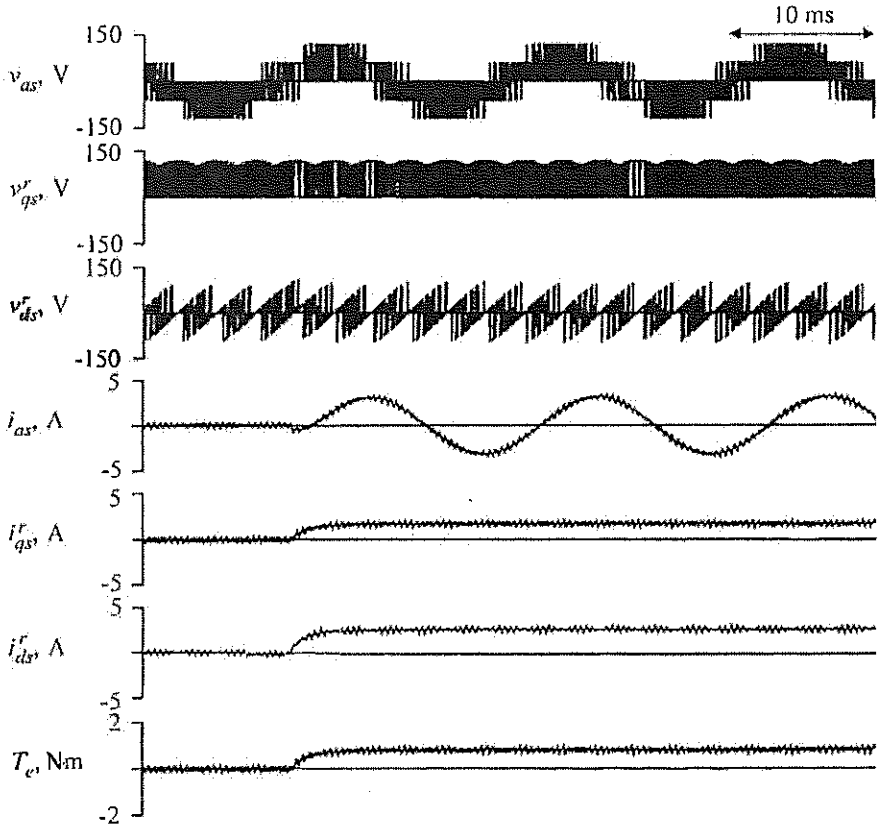

Figure 15B-1 Step response of a feedforward current-regulated sine-triangle modulated brushless dc motor drive.

the effect of the back emf, and a proportional-plus-integral (PI) control loop to drive the error to zero. Assuming that the actual q- and d-axis voltages are equal to the commanded q- and d-axis voltages, it can be shown that the transfer function between the commanded and actual q-axis currents is given by

$$\frac{i^r_{qs}(s)}{i^{r*}_{qs}(s)} = \frac{\frac{K_p}{L_{ss}}\left(s + \frac{K_i}{K_p}\right)}{s^2 + \frac{(r_s + K_p)}{L_{ss}}s + \frac{K_i}{L_{ss}}} \tag{15B-3}$$

The transfer function relating the d-axis current to the commanded d-axis current is identical. Assuming the same machine parameters as in the study illustrated in Fig. 15.9-2, and selecting pole locations of $s = -200$ and $s = -1000$ (note that the poles may be arbitrarily placed), we have that

$$K_i = 2280\,\Omega/s \tag{15B-4}$$

$$K_p = 10.7\,\Omega \tag{15B-5}$$

Figure 15B-1 illustrates the response of the brushless dc drive as the current command is stepped from zero to $i^{r*}_{qs} = 1.73$ A and $i^{r*}_{ds} = 2.64$ A. All operating conditions are as in Fig. 15.9-2. As can be seen, the machine performance is extremely well behaved and is dominated by the pole at $s = -200$.

15.10 VOLTAGE LIMITATIONS OF CURRENT-SOURCE INVERTER DRIVES

As alluded to previously, assuming that the current control loop is sufficiently fast, the current-regulated drive can be thought of as an ideal current source. However, there are some limitations on the validity of this approximation. In particular, eventually the back emf of the machine will rise to the point where the inverter cannot supply the current commands due to the fact that the back emf of the machine becomes too large. Under such conditions, the machine is said to have lost current tracking.

In order to estimate the operating region over which current tracking is obtained, note that if it is obtained we have

$$\bar{i}^r_{qs} = i^{r*}_{qs} \tag{15.10-1}$$

$$\bar{i}^r_{ds} = i^{r*}_{ds} \tag{15.10-2}$$

Substituting (15.10-1) and (15.10-2) into the stator voltage equations and neglecting the stator dynamics yields

$$\bar{v}^r_{qs} = r_s i^{r*}_{qs} + \omega_r L_d i^{r*}_{ds} + \omega_r \lambda'_m \tag{15.10-3}$$

$$\bar{v}^r_{ds} = r_s i^{r*}_{ds} - \omega_r L_q i^{r*}_{qs} \tag{15.10-4}$$

Recall that the rms value of the fundamental component of the applied voltage is given by

$$v_s = \frac{1}{\sqrt{2}}\sqrt{\left(\bar{v}_{qs}^{r}\right)^2 + \left(\bar{v}_{ds}^{r}\right)^2} \tag{15.10-5}$$

Substitution of (15.10-3) and (15.10-4) into (15.10-5) yields

$$v_s = \frac{1}{\sqrt{2}}\sqrt{\left(r_s i_{qs}^{r*} + \omega_r L_d i_{ds}^{r*} + \lambda_m' \omega_r\right)^2 + \left(r_s i_{ds}^{r*} - \omega_r L_q i_{qs}^{r*}\right)^2} \tag{15.10-6}$$

Recall from Section 13.8 that for the hysteresis-modulated current-regulated inverters, the maximum rms value of the fundamental component of the applied voltage which can be obtained without low-frequency harmonics is given by

$$v_s = \frac{1}{\sqrt{6}}\bar{v}_{dc} \tag{15.10-7}$$

If low-frequency harmonics are tolerable and a synchronous regulator is used, either in the context of a sine-triangle voltage-source inverter-based current loop or with the hysteresis-modulated current regulator, then the maximum rms value of the fundamental component becomes

$$v_s = \frac{\sqrt{2}}{\pi}\bar{v}_{dc} \tag{15.10-8}$$

In the event that for a given current command and speed (15.10-8) cannot be satisfied, then it is not possible to obtain stator currents equal to the commanded currents. If (15.10-8) can be satisfied, but (15.10-7) cannot be satisfied, then it is possible to obtain stator currents that have the same fundamental component as the commanded currents provided that integral feedback in the rotor reference frame is present to drive the current error to zero. However, low-frequency harmonics will be present.

Figure 15.10-1 illustrates the effects of loss of current tracking. Initially, operating conditions are identical to those portrayed in Fig. 15.9-2. However, approximately 20 ms into the study, the dc inverter voltage is stepped from 177 V to 124 V, which results in a loss of current tracking. As can be seen, the switching of the hysteresis current regulator is such that some compensation takes place; nevertheless current tracking is lost. As a result, harmonics appear in the a-phase and q- and d-axis current waveforms, as well as in the electromagnetic torque.

15.11 CURRENT COMMAND SYNTHESIS

It is now appropriate to address the question as to how to determine the current command. Normally, when using a current-regulated inverter, the input to the

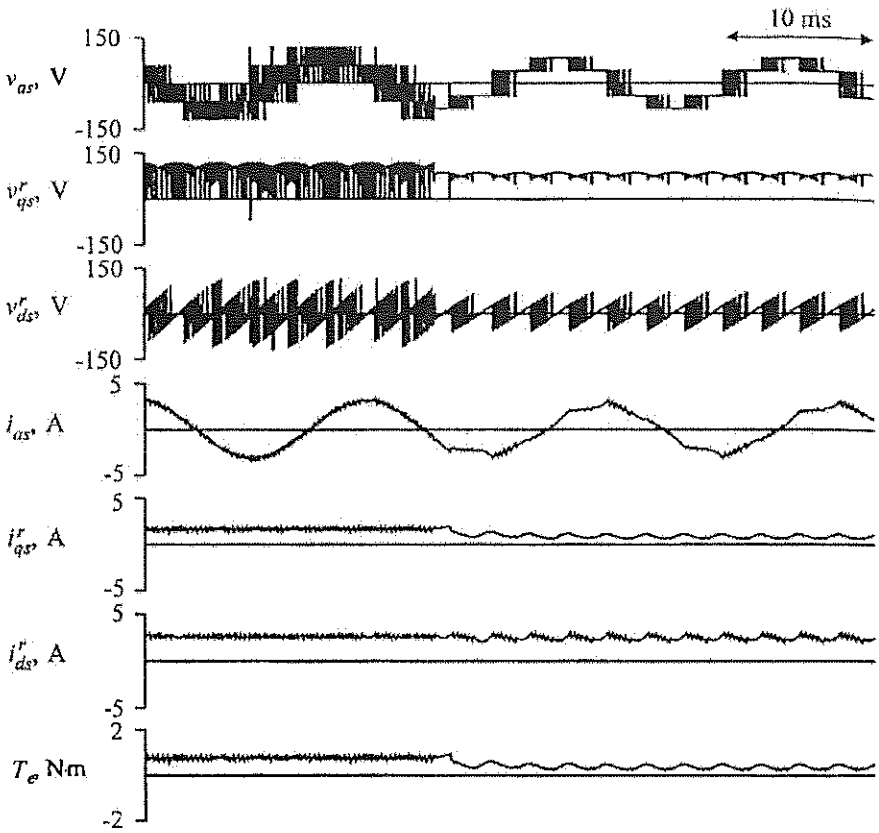

Figure 15.10-1 Response of hysteresis-modulated brushless dc motor drive to step decrease in dc inverter voltage.

controller is a torque command. Thus, the problem may be reformulated as the determination of the current command from the torque command. To answer this question, let us first consider a nonsalient machine in which $L_q = L_d$. From (6.3-14), torque may be expressed as

$$T_e = \frac{3}{2}\frac{P}{2}\lambda'_m i'_{qs} \tag{15.11-1}$$

Therefore, the commanded q-axis current may be expressed in terms of the commanded torque as

$$i'^{*}_{qs} = \frac{2}{3}\frac{2}{P}\frac{1}{\lambda'_m}T^{*}_e \tag{15.11-2}$$

Clearly, if the desired torque is to be obtained, then (15.11-2) must be satisfied. The d-axis current does not affect average torque, and so its selection is somewhat

arbitrary. Because d-axis current does not affect the electromagnetic torque, but does result in additional stator losses, it is often selected to be zero, that is,

$$i_{ds}^{r*} = 0 \tag{15.11-3}$$

This selection of d-axis current minimizes the current amplitude into the machine, thus maximizing torque-per-amp and at the same time maximizing the efficiency of the machine by minimizing the stator resistive losses.

Although (15.11-3) has several distinct advantages, there is one reason to command a nonzero d-axis current. To see this reason, consider (15.10-6) for the nonsalient case:

$$v_s = \frac{1}{\sqrt{2}}\sqrt{\left(r_s i_{qs}^{r*} + \omega_r L_{ss} i_{ds}^{r*} + \lambda_m' \omega_r\right)^2 + \left(r_s i_{ds}^{r*} - \omega_r L_{ss} i_{qs}^{r*}\right)^2} \tag{15.11-4}$$

From (15.11-4) we see that the required inverter voltage goes up with speed and with q-axis current (which is proportional to torque). However, when we examine the first squared term in (15.11-4), it can be seen that at positive speeds the required inverter voltage can be reduced by injecting negative d-axis current. In fact, by solving (15.11-4) for d-axis current in terms of the q-axis current command and speed, we have that the d-axis current injection that allows us to operate within the voltage constraint is given by

$$i_{ds}^{r*} = \frac{-\lambda_m' L_{ss}\omega_r^2 + \sqrt{2z^2 v_s^2 - \left(r_s \omega_r \lambda_m' + z^2 i_{qs}^{r*}\right)^2}}{z^2} \tag{15.11-5}$$

where

$$z = \sqrt{r_s^2 + \omega_r^2 L_{ss}^2} \tag{15.11-6}$$

Thus, a logical current control strategy is to command zero d-axis current as long as the inverter voltage requirements are not exceeded, and to inject the amount of d-axis current specified by (15.11-5) if they are. Note that there are limitations on d-axis current injection in that (i) (15.11-5) may not have a solution, (ii) excessive d-axis current injection may result in demagnetization of the permanent magnet, and (iii) excessive d-axis current injection can result in exceeding the current limit of the machine or inverter. In addition, the use of (15.11-5) requires accurate knowledge of the dc inverter voltage (to determine the peak v_s), the rotor speed, and all of the machine parameters. A means of implementing such a control without knowledge of the dc inverter voltage, speed, and machine parameters is set forth in reference 8.

The process for determining the current command in salient machines, which typically are constructed using buried-magnet technology, is somewhat more involved than in the nonsalient case. Let us first consider the problem of computing the q- and d-axis current commands so as to maximize torque-per-amp performance.

In the case of the salient machine, from Chapter 6 the expression for electromagnetic torque is given by

$$T_e = \frac{3}{2}\frac{P}{2}(\lambda'_m i^r_{qs} + (L_d - L_q) i^r_{qs} i^r_{ds}) \tag{15.11-7}$$

Solving (15.11-7) for d-axis current command in terms of the q-axis current command and in terms of the commanded torque yields

$$i^{r*}_{ds} = \frac{T_e}{\frac{3}{2}\frac{P}{2}(L_d - L_q)} \frac{1}{i^{r*}_{qs}} - \frac{\lambda'_m}{L_d - L_q} \tag{15.11-8}$$

In terms of the q- and d-axis current commands, the rms value of the fundamental component of the commanded current is given by

$$i_s = \frac{1}{\sqrt{2}} \sqrt{(i^{r*}_{qs})^2 + (i^{r*}_{ds})^2} \tag{15.11-9}$$

Substitution of (15.11-8) into (15.11-9) yields an expression for the magnitude of the stator current in terms of the commanded torque and q-axis current command. Setting the derivative of the resulting expression with respect to the q-axis current command equal to zero yields the following transcendental expression for the q-axis current command:

$$(i^{r*}_{qs})^4 + \frac{T_e \lambda'_m i^{r*}_{qs}}{\frac{3}{2}\frac{P}{2}(L_d - L_q)^2} - \left(\frac{T_e}{\frac{3}{2}\frac{P}{2}(L_d - L_q)}\right)^2 = 0 \tag{15.11-10}$$

The solution of (15.11-10) yields the value of q-axis current that maximizes torque-per-amp performance. Once the q-axis current command is determined by solving (15.11-10), the d-axis current command may be found by solving (15.11-8). From the form of (15.11-10), it is apparent that the solution for the q-axis current must be accomplished numerically. For this reason, when implementing this control with a microprocessor, the q- and d- axis current commands are often formulated through a table look-up that has been constructed by solving (15.11-8) and (15.11-10) offline.

Once the q- and d-axis current commands have been formulated, it is necessary to check whether or not the inverter is capable of producing the required voltage. If it is not, it is necessary to recalculate the commanded q- and d-axis currents such that the required inverter voltage does not exceed that obtainable by the converter. This calculation can be conducted by solving (15.10-6) and (15.11-8) simultaneously for the q- and d-axis current command.

Figure 15.11-1 illustrates the graphical interpretation of the selection of the commanded q- and d-axis currents for a machine in which $r = 0.2\ \Omega$, $L_q = 20$ mH, $L_d = 10$ mH, and $\lambda'_m = 0.07$ V·s. The machine is operating at a speed of

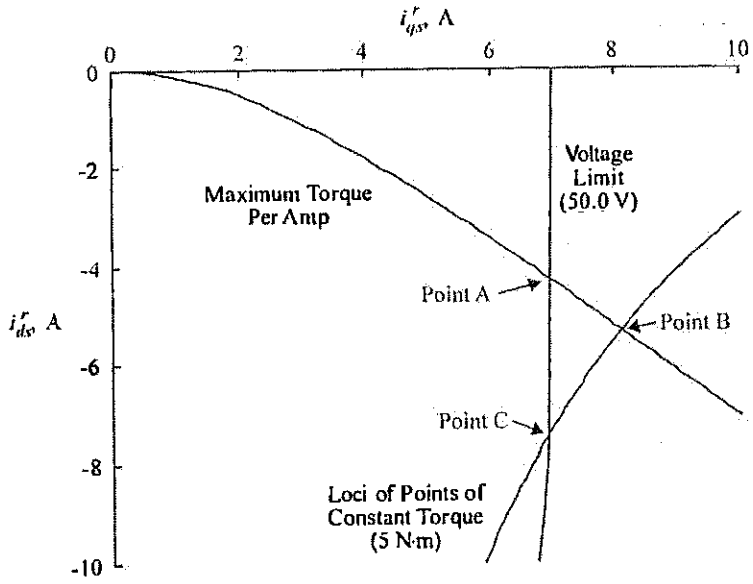

Figure 15.11-1 Selection of q- and d-axis current trajectory.

500 rad/s (electrical) and $v_s = 50$ V. Illustrated therein are the trajectory of the maximum torque-per-amp characteristic, the loci of points in the q- and d-axis current plane at which the electromagnetic torque of 5 N · m is obtained, and the loci of points representing the voltage limit imposed by (15.10-6). For a given electromagnetic torque command, the q- and d-axis current command is formulated using the maximum torque-per-amp trajectory, provided that this point is inside the voltage limit. However, q- and d-axis currents on this trajectory corresponding to torques greater than that obtainable at point A cannot be achieved if the q- and d-axis current is confined to the maximum torque-per-amp trajectory. Suppose a torque of 5 N · m is desired. Point B represents the point on this maximum torque-per-amp trajectory which has the desired torque. Unfortunately, point B is well outside of the limit imposed by the available voltage. However, note that any point on the constant torque locus will satisfy the desired torque. Thus, in this case the current command is chosen to correspond to point C.

15.12 AVERAGE-VALUE MODELING OF CURRENT-REGULATED INVERTER DRIVES

In this section, an average-value model of current-regulated and current-source inverter drives is formulated in much the same way as the average-value model of voltage-source inverter drives. Because the topology of the converter has not changed, it follows that the expressions for the time derivatives of the rectifier current, the

dc link voltage, the stabilizing filter current, and the stabilizing filter voltage given by (15.4-6)–(15.4-9) are valid. Furthermore, the change in control strategy does not affect the mechanical dynamics, thus (15.4-14) and (15.4-15) may still be used to represent the machine. However, the change in control strategy will change the formulation of the expression for the dc link currents, the stator dynamics, and the expression for electromagnetic torque.

In order to formulate an expression for the dc link current, it is convenient to assume that the actual machine currents are equal to the commanded machine currents whereupon

$$\bar{i}'_{qs} = i'^{*}_{qs} \tag{15.12-1}$$

$$\bar{i}'_{ds} = i'^{*}_{ds} \tag{15.12-2}$$

Of course, this assumption is only valid when the dc link voltage is such that the desired current is actually obtained. An average-value model of brushless dc drives in which the current tracking is not obtained is set forth in reference 9. Assuming that the actual currents are equal to the commanded currents, the stator currents are no longer state variables. Neglecting the stator dynamics, the q- and d-axis voltages may be expressed as

$$\bar{v}'^{*}_{qs} = r_s i'^{*}_{qs} + \omega_r L_d i'^{*}_{ds} + \lambda'_m \omega_r \tag{15.12-3}$$

$$\bar{v}'_{ds} = r_s i'^{*}_{ds} - \omega_r L_q i'^{*}_{qs} \tag{15.12-4}$$

The instantaneous power into the machine is given by

$$P = \frac{3}{2}[r_s(i'^{*}_{qs} + i'^{*}_{ds})^2 + \omega_r(L_d - L_q)i'^{*}_{qs} i'^{*}_{ds} + \omega_r \lambda'_m i'_{qs}] \tag{15.12-5}$$

Assuming that no power is lost into the inverter, if follows that the dc link current is given by

$$\bar{i}_{dc} = \frac{\bar{P}}{\bar{v}_{dc}} \tag{15.12-6}$$

Combining (15.12-5) with (15.12-6) yields

$$\bar{i}_{dc} = \frac{3}{2}\frac{1}{\bar{v}_{dc}}[r_s(i'^{*}_{qs} + i'^{*}_{ds})^2 + \omega_r(L_d - L_q)i'^{*}_{qs} i'^{*}_{ds} + \omega_r \lambda'_m i'_{qs}] \tag{15.12-7}$$

The other expression affected by the change from a voltage-source inverter to a current-source or current-regulated inverter will be the expression for torque. In particular, from (15.4-12) and again assuming that the actual stator currents are equal to the commanded currents, we obtain

$$\bar{T}_e = \frac{3}{2}\frac{P}{2}(\lambda'_m i'^{*}_{qs} + (L_d - L_q)i'^{*}_{qs} i'^{*}_{ds}) \tag{15.12-8}$$

As can be seen from (15.12-8), if it is assumed that the actual currents are equal to the commanded currents, then any desired torque may be instantaneously obtained.

Combining (15.4-7), (15.4-10), (15.4-11), (15.4-12), (15.4-19), (15.12-7), and (15.12-8) yields

$$p\begin{bmatrix} \bar{i}_r \\ \bar{v}_{dc} \\ \bar{i}_{st} \\ \bar{v}_{st} \\ \omega_r \end{bmatrix} = \begin{bmatrix} -\frac{r_{st}}{L_{st}} & -\frac{1}{L_{st}} & 0 & 0 & 0 \\ \frac{1}{C_{dc}} & 0 & -\frac{1}{C_{dc}} & 0 & 0 \\ 0 & \frac{1}{L_{st}} & -\frac{r_{st}}{L_{st}} & -\frac{1}{L_{st}} & 0 \\ 0 & 0 & \frac{1}{C_{st}} & 0 & 0 \\ 0 & 0 & 0 & 0 & 0 \end{bmatrix} \begin{bmatrix} \bar{i}_r \\ \bar{v}_{dc} \\ \bar{i}_{st} \\ \bar{v}_{st} \\ \omega_r \end{bmatrix} + \begin{bmatrix} \frac{v_{s0}\cos\alpha}{L_{st}} \\ -\frac{1}{C_{dc}}\frac{3}{2}\frac{1}{V_{dc}}\left[r_s\left(i_{qs}^{r*}+i_{ds}^{r*}\right)^2+\omega_r(L_{sd}-L_{sq})i_{qs}^{r*}i_{ds}^{r*}+\omega_r\lambda_m' i_{qs}^{r*}\right] \\ 0 \\ 0 \\ \frac{P}{2}\frac{1}{J}\left[\frac{3}{2}\frac{P}{2}\left(\lambda_m' i_{qs}^{r*}+(L_{sd}-L_{sq})i_{qs}^{r*}i_{ds}^{r*}\right)-T_L\right] \end{bmatrix} \tag{15.12-9}$$

15.13 CASE STUDY: CURRENT-REGULATED INVERTER-BASED SPEED CONTROLLER

The control of current-regulated inverter-based drives is considerably simpler than its voltage-source-based counterpart, due to the fact that when designing the speed or position control algorithms, the inverter and machine may be modeled as a nearly ideal torque transducer (neglecting the stator dynamics of the machine). To illustrate this, let us reconsider the speed control system discussed in Section 15.8. Assuming that a current command synthesizer and current regulator can be designed with sufficiently high bandwidth, the speed control algorithm may be designed by assuming that the drive will produce an electromagnetic torque equal to the desired torque,

$$T_e = T_e^* \tag{15.13-1}$$

In order to ensure that there will be no steady-state error, let's propose a PI control law in accordance with (15.12-2):

$$T_e^* = K_p\left(1+\frac{1}{\tau s}\right)(\omega_{rm}^* - \omega_{rm}) \tag{15.13-2}$$

wherein ω_{rm}^* represents the speed command. Combining (15.13-1), (15.13-2), and the mechanical dynamics of the drive, it can be shown that the resulting transfer function between the actual and commanded rotor speed is given by

$$\frac{\omega_{rm}}{\omega_{rm}^*} = \frac{\frac{K}{J\tau}(\tau s+1)}{s^2+\frac{K}{J}s+\frac{K}{J\tau}} \tag{15.13-3}$$

Because (15.13-3) represents a second-order system and there are two free parameters, the poles of (15.13-3) may be arbitrarily placed. However, some restraint should be exercised because it is important that the current regulator be much faster than the mechanical system if (15.13-1) and hence (15.13-3) are to remain valid. Placing the poles at $s = -5$ and $s = -50$ yields $K = 0.257$ N·m·s/rad and $\tau = 0.22$ s. The pole at $s = -5$ will dominate the response.

In order to complete the design, a current command synthesizer (to determine what the current command should be to achieve the desired torque) and a current regulation control strategy need to be designed. For this example, let us assume a simple current command synthesizer in which all of the current is injected into the q-axis, and let us use the sine-triangle-based current regulator set forth in Example 15B as a current regulator. Recall that the poles of the current regulator are at $s = -200$ and $s = -1000$, which are much faster than those of the mechanical system.

Practically speaking, there are two important refinements that can be made to this control system. First, the q-axis current command generated by the current command synthesizer should be limited to ± 3.68 A in order to limit the current to the rated value of the machine. In order to avoid the current limit from causing windup of the speed control integrator, the contribution of the $K/(\tau s)$ portion of the speed control (that is the integral portion of the control) should be limited. Herein, the portion of the torque command contributed by the integral term will be limited so that the overshoot under worst-case conditions is limited to an acceptable value (some trial and error using dynamic simulations would be used to determine the exact number).

Figure 15.13-1 illustrates the interactions of the various controllers. Based on the speed error, the PI speed control determines a torque command T_e^* (the limit on the integral feedback is not shown). Then the current command synthesizer determines the q-axis current required to obtain the desired torque, subject to the q-axis current limit. In this controller, the d-axis current is set at zero. Based on the commanded q- and d-axis currents, the electrical rotor speed, the actual currents, and the dc

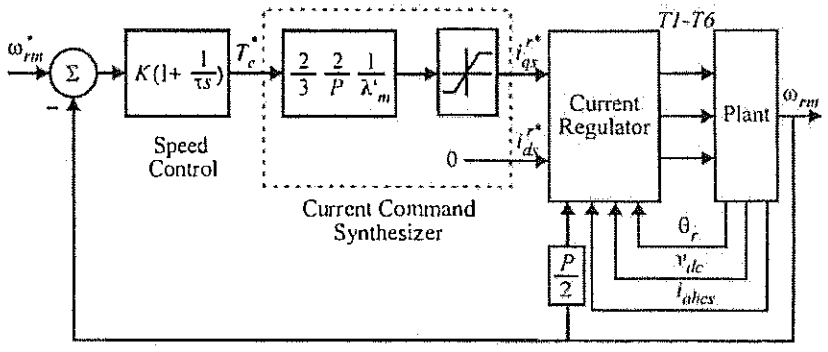

Figure 15.13-1 Current-regulated inverter-based speed control.

supply voltage of the current regulator determines the on or off status of each of the semiconductors in the inverter (T1–T6).

Figure 15.13-2 illustrates the performance of the speed control system. Initially the system is in the steady-state. However, 50 ms into the study the speed command is stepped from 0 to 200 rad/s. As can be seen, the torque command immediately jumps to the value that corresponds to the maximum q-axis current command. Because the electromagnetic torque is constant, the speed increases linearly with time. As can be seen, the magnitude of the ac current into the rectifier and the rectifier current both increase linearly with speed. This is due to the fact that the power going into the machine increases linearly with speed. The increasing rectifier current results in a dc inverter voltage that decreases linearly with time. Note that the dc link voltage initially undergoes a sudden dip of 5 V that we might not have expected; this is due to the fact that initially the rectifier was under no-load condition and hence charged the dc link capacitor to peak rather than average value of the rectifier voltage. Eventually, the machine reaches the desired speed. At this point the torque command falls off because the load is inertial. As a result, the electromagnetic torque, stator current, and rectifier current all decrease to their original values, and the dc inverter voltage increases to its original value. Comparing Fig. 15.13-2 to Fig. 15.8-5, the reader will observe that the current-based speed control system is

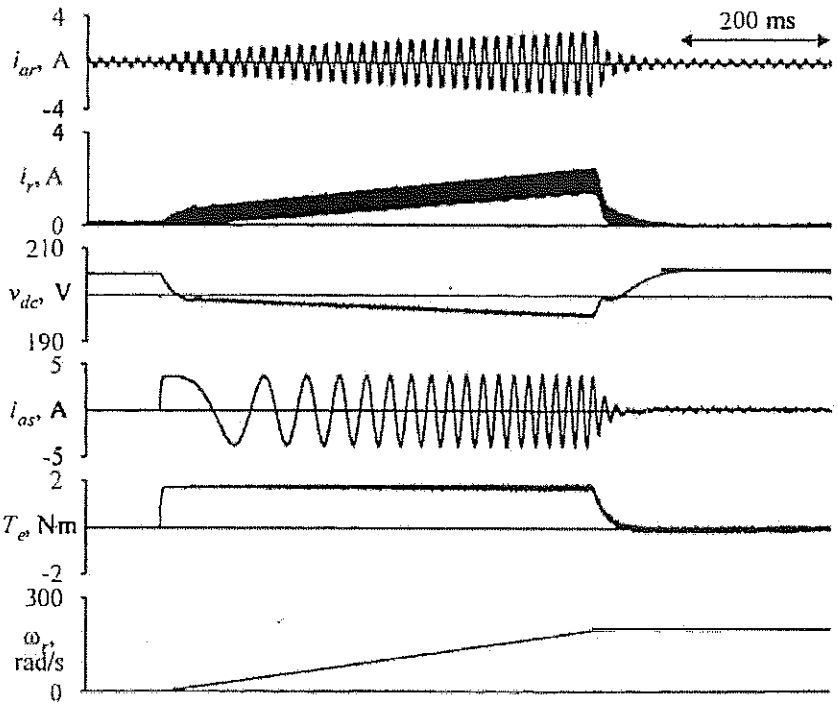

Figure 15.13-2 Start-up response of current-regulated inverter-based speed control system.

considerably more sluggish than the voltages-source-based speed control system. However, this is a result of the fact that the current-regulated inverter-based system did not exceed the current limits of the machine. In fact, the current-regulated inverter-based system brought the machine to the commanded speed as fast as possible subject to the limitation of the stator current.

REFERENCES

[1] P. L. Chapman, S. D. Sudhoff, and C. Whitcomb, Multiple Reference Frame Analysis of Non-Sinusoidal Brushless DC Drives, ***IEEE Transactions on Energy Conversion***, Vol. 14., No. 3, September 1999, pp 440–446.

[2] P. L. Chapman, S. D. Sudhoff, and C. A. Whitcomb, Optimal Current Control Strategies for Non-Sinusoidal Permanent-Magnet Synchronous Machine Drives, ***IEEE Transactions on Energy Conversion***, Vol. 14, No. 3, December 1999, pp. 1043–1050.

[3] P. L. Chapman and S. D. Sudhoff, A Multiple Reference Frame Synchronous Estimator/Regulator, ***IEEE Transactions on Energy Conversion***, Vol. 15, No. 2. June 2000, pp. 197–202.

[4] B. T. Kuhn, S. D. Sudhoff, and C. A. Whitcomb, Performance Characteristics and Average-Value Modeling of Auxiliary Resonant Commutated Pole Converter Based Induction Motor Drives, ***IEEE Transactions on Energy Conversion***, Vol. 14. No. 3, September 1999, pp. 493–499.

[5] H. G. Yeo, C. S. Hong, J. Y. Yoo, H. G. Jang, Y. D. Bae, and Y. S. Park, Sensorless Drive for Interior Permanent Magnet Brushless DC Motors, ***IEEE International Electric Machines and Drives Conference Record***, May 18–21, 1997, pp. TDI-3.1–TD1-3.3.

[6] K. A. Corzine and S. D. Sudhoff, A Hybrid Observer for High Performance Brushless DC Drives, ***IEEE Transactions on Energy Conversion***, Vol. 11, No. 2, June 1996, pp. 318–323.

[7] T. M. Rowan and R. J. Kerkman, A New Synchronous Current Regulator and an Analysis of Current-Regulated Inverters, ***IEEE Transactions on Industry Applications***, Vol. IA-22, No. 4, 1986, pp. 678–690.

[8] S. D. Sudhoff, K. A. Corzine, and H. J. Hegner, A Flux-Weakening Strategy for Current-Regulated Surface-Mounted Permanent-Magnet Machine Drives, ***IEEE Transactions on Energy Conversion***, Vol. 10, No. 3, September 1995, pp. 431–437.

[9] K. A. Corzine, S. D. Sudhoff, and H. J. Hegner, Analysis of a Current-Regulated Brushless DC Drive, ***IEEE Transactions on Energy Conversion***, Vol. 10, No. 3, September 1995, pp. 438–445.

PROBLEMS

1 Consider the brushless dc drive whose characteristics are depicted in Fig. 15.5-1. Plot the characteristics if the phase delay is in accordance with (6.4-24).

2 Repeat Problem 1, except at each speed calculate the phase delay which maximizes torque [which is *not* given by (14.4-7)].

3 Consider the drive system whose parameters are given in Table 15.8-1. If the phase delay is to be set equal to zero, compute the turns ratio of the transformer with the minimum